NAVAL POSTGRADUATE SCHOOL
MONTEREY, CALIFORNIA

THESIS

PARAMETRICS OF NEAR SURFACE RESPONSE OF SUBMERSIBLE VEHICLES

by

A. Kaan Çelikel

September, 1996

Thesis Advisor: Fotis A. Papoulias

Approved for public release; distribution is unlimited.

DISCLAIMER NOTICE

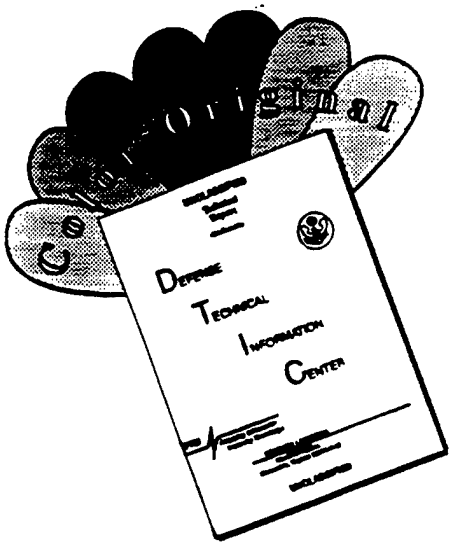

THIS DOCUMENT IS BEST QUALITY AVAILABLE. THE COPY FURNISHED TO DTIC CONTAINED A SIGNIFICANT NUMBER OF COLOR PAGES WHICH DO NOT REPRODUCE LEGIBLY ON BLACK AND WHITE MICROFICHE.

REPORT DOCUMENTATION PAGE

Form Approved OMB No. 0704-0188

1. AGENCY USE ONLY *(Leave blank)*	2. REPORT DATE September 1996	3. REPORT TYPE AND DATES COVERED Master's Thesis

4. TITLE AND SUBTITLE
PARAMETRICS OF NEAR SURFACE RESPONSE OF SUBMERSIBLE VEHICLES

5. FUNDING NUMBERS

6. AUTHOR(S) A. Kaan Çelikel

7. PERFORMING ORGANIZATION NAME(S) AND ADDRESS(ES)
Naval Postgraduate School
Monterey CA 93943-5000

8. PERFORMING ORGANIZATION REPORT NUMBER

9. SPONSORING/MONITORING AGENCY NAME(S) AND ADDRESS(ES)

10. SPONSORING/MONITORING AGENCY REPORT NUMBER

11. SUPPLEMENTARY NOTES The views expressed in this thesis are those of the author and do not reflect the official policy or position of the Department of Defense or the U.S. Government.

12a. DISTRIBUTION/AVAILABILITY STATEMENT
Approved for public release; distribution is unlimited.

12b. DISTRIBUTION CODE

13. ABSTRACT *(maximum 200 words)* Vertical plane response of submersible vehicles in the proximity of a free surface in deep water is evaluated using a potential flow, strip theory solver. Two criteria, that are periscope submergence, and sail broaching are used to quantify the response. These criteria combined with the vehicle's response amplitude operators in regular sinusoidal waves along with a statistical description of the seaway lead to an assessment of an overall operability index for the vehicle. This thesis presents a systematic parametric study of the effects of body geometry on near surface response. Two cases, namely limited diameter and limited length are considered. The total volume of the vehicle is kept constant, and certain shape factors are changed, while either the overall diameter or the overall length remains the same. The operability index is calculated for each case within a given range for sea states and sea directions and for various shape factors, vehicle speeds and operating depths. The results indicate that certain changes of shape factors can improve vehicle operations in various depth and speed combinations.

14. SUBJECT TERMS SUBMERSIBLE VEHICLES, PERISCOPE DEPTH OPERATIONS, OPERABILITY INDEX, STRIP THEORY

15. NUMBER OF PAGES 87

16. PRICE CODE

17. SECURITY CLASSIFICATION OF REPORT	18. SECURITY CLASSIFICATION OF THIS PAGE	19. SECURITY CLASSIFICATION OF ABSTRACT	20. LIMITATION OF ABSTRACT
Unclassified	Unclassified	Unclassified	UL

NSN 7540-01-280-5500
Standard Form 298 (Rev. 2-89)
Prescribed by ANSI Std. 239-18 298-102

Approved for public release; distribution is unlimited.

PARAMETRICS OF NEAR SURFACE RESPONSE OF SUBMERSIBLE VEHICLES

A. Kaan Çelikel
LTJG, Turkish Navy
B.S., Turkish Naval Academy - 1989

Submitted in partial fulfillment
of the requirements for the degree of

MASTER OF SCIENCE IN MECHANICAL ENGINEERING

from the

NAVAL POSTGRADUATE SCHOOL
September 1996

Author: _____
A. Kaan Çelikel

Approved by: _____
Fotis A. Papoulias , Thesis Advisor

_____
Terry R. McNelley, Chairman
Department of Mechanical Engineering

ABSTRACT

Vertical plane response of submersible vehicles in the proximity of a free surface in deep water is evaluated using a potential flow, strip theory solver. Two criteria, that are periscope submergence, and sail broaching are used to quantify the response. These criteria combined with the vehicle's response amplitude operators in regular sinusoidal waves along with a statistical description of the seaway lead to an assessment of an overall operability index for the vehicle. This thesis presents a systematic parametric study of the effects of body geometry on near surface response. Two cases, namely limited diameter and limited length are considered. The total volume of the vehicle is kept constant, and certain shape factors are changed, while either the overall diameter or the overall length remains the same. The operability index is calculated for each case within a given range for sea states and sea directions and for various shape factors, vehicle speeds and operating depths. The results indicate that certain changes of shape factors can improve vehicle operations in various depth and speed combinations.

TABLE OF CONTENTS

I. INTRODUCTION.....1

II. EVALUATION OF RESPONSE.....5

A. GEOMETRY OF A SUBMARINE.....5

B. MOTIONS IN A SEAWAY.....10

III. RESULTS.....17

A. OPERABILITY INDEX.....17

B. PERISCOPE SUBMERGENCE CRITERION RESULTS 20

C. SAIL BROACHING CRITERION RESULTS 35

D. COMBINED CRITERIA RESULTS 50

IV. CONCLUSIONS AND RECOMMENDATIONS.....65

A. CONCLUSIONS.....65

B. RECOMMENDATIONS.....66

APPENDIX PROGRAMS.....67

LIST OF REFERENCES.....73

INITIAL DISTRIBUTION LIST.....75

ACKNOWLEDGEMENT

I would like to thank my thesis advisor, Professor Fotis A. Papoulias, for his guidance in this thesis research.

I. INTRODUCTION

Submarine periscope depth operations are conducted in order to accomplish specific tasks and perform them in minimum time and with the least amount of noise. Accurate submarine maneuvering predictions are essential both for design to assess alternatives based on their maneuvering performance, and for operation, to provide optimal and safe submerged operating envelopes. Submarines are subject to several exciting forces and moments at periscope depth beneath a seaway. These forces and moments induce an oscillatory motion at the wave frequencies and second-order drifting motions at very low frequencies well outside the wave spectrum of the seaway, which are referred to as free surface suction effects. It is difficult in practice to control these low frequency motions and may result in a rise to unsatisfactory depth keeping. Standard ways of computing free surface effects rely on combinations of potential flow and semi-empirical coefficient based models. Rankine type sources are distributed along the hull of the ship, which satisfy the free surface boundary condition. Source strength can be computed by satisfying the exact body boundary condition, that no fluid can pass through the hull surface. Discretization of the hull form into a finite set of Hess-Smith type quadrilateral panels allows formulation of algebraic system of equations to be solved for the unknown singularity strengths [Ref. 1]. Combination of forces and moments generated in this way with deep water force predictions can then be utilized to simulate the motion of the boat under waves. These forces and moments are slowly varying in time and as a result they can be controlled by either the operators or automatic control systems. In this work a

potential flow, strip theory solver program is utilized to determine vehicle motions in the proximity of a free surface in deep water, based on the work by Beck and Troesch [Ref. 2].

Tactical assessment is possible by adopting a number of criteria, each pertaining to different operational hazards. These criteria can be divided into two main categories, such as subtle and catastrophic failures. In the study, we have considered two criteria which are periscope submergence and sail broaching. Periscope submergence is a subtle failure and sail broaching is a catastrophic failure.

Subtle failures are the events which will occur in all types of periscope depth operations, such as, propeller emergence, mast emergence, periscope submergence, mast submergence. The frequency of these events imposes operability limits for a certain sea-state, although single occurrence of them does not constitute failure of operations. Periscope submergence impairs visual information. The dominant criterion is the number of occurrences per unit time.

Catastrophic failures are the ones which will probably result in either cancel of operations, failure to complete mission or submarine detection, such as sail broaching, loss of depth control deep. Since a single event occurrence is identified as a catastrophic failure, the primary analytical criterion is the expected duration between two consecutive events, instead of being the number of events per time. Broaching is defined as the loss of depth control shallow to a sufficient extent and duration. It is assumed that the submarine detection will occur with probability of one each time a broaching occurs.

In Chapter II of the thesis, evaluation of the response is described, beginning with the definition of submarine geometry. A typical hull consists of three sections, the entrance (bow) the shape of a parabolic body of revolution, the parallel middle body of a cylindrical shape, and the run (stern) the shape of an ellipsoid of revolution (Jackson,1992) [Ref. 3]. The parameters and all the coefficients are explained and formulated. Chapter III shows the resulting operability indexes of a submarine for different sea-states and wave heading angles and deep water operations for periscope submergence, sail broaching and combined criteria. These results are obtained from the limited diameter and limited length cases, different shape factors and speed/operating depth combinations. Conclusions from the study and recommendations for further studies are presented in Chapter IV.

II. EVALUATION OF RESPONSE

A. GEOMETRY OF A SUBMARINE

A typical submarine hull is considered as a generic body of revolution, which is rotated about a line parallel to the center-line, as described by Jackson (1992) [Ref. 3]. It has a length/diameter (L/D) ratio of six and a maximum diameter at $0.4L$. The body is composed of three main sections, as shown in Figure 1 [Ref. 3]. The forward section is called the entrance, which is a portion of an ellipsoid of revolution. The middle section is the parallel middle body (PMB) with a cylindrical shape. The third section is the after end called the run, which is composed of a paraboloid of revolution. The entrance has a length, L_f, of 2.4 diameters. The run has a length, L_a, of 3.6 diameters. The algebraic sum of the lengths, L_f, L_a, and the length of the PMB, L_{PMB}, is the overall length of the hull.

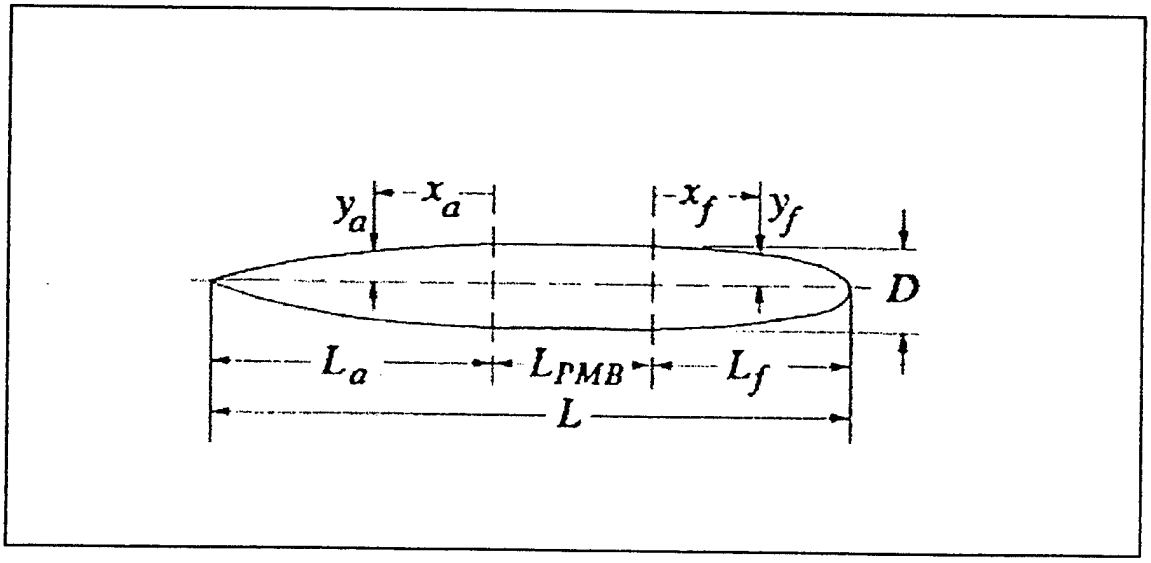

Figure 1. Submarine Geometry [Ref. 3]

The body coordinates, which define the forward and aft shapes are given by,

$$y_f = \frac{D}{2}\left[1-\left(\frac{x_f}{L_f}\right)^{n_f}\right]^{1/n_f} \quad (1)$$

$$y_a = \frac{D}{2}\left[1-\left(\frac{x_a}{L_a}\right)^{n_a}\right] \quad (2)$$

The values of x_f and x_a are the offsets from the maximum diameter, and y_f and y_a are the radii at the respective offset points.

The exponents (n_a and n_f) in Equations (1) and (2) are the shape factor coefficients, which control the shape of the fore and aft bodies, respectively. Higher values of these coefficients correspond to fuller hull shapes, and lower values to finer shapes. The effects of changing the shape factor coefficients on the hull shape are shown in Figures 2 and 3, where the hull shapes for three values of the shape factors 2, 3 and 4 are shown. In this study, it is assumed that the total volume of the ship remains the same (so that ship displacement does not vary), while either overall length or diameter remains the same. We refer to the first case as the limited length case or inactive diameter constraint, and to the second case as the limited diameter case or inactive length constraint. Both of these two cases will be analyzed in our parametric studies.

If one were to use equations for true ellipsoids and parabolas, the entrance and the run would be too fine for a modern submarine. The displacement can be increased by using larger shape factors or higher L_{PMB}. The prismatic coefficients , C_{pa} and C_{pf} ,are used to calculate volumes. For a cylinder its prismatic coefficient is 1. For a submarine-like

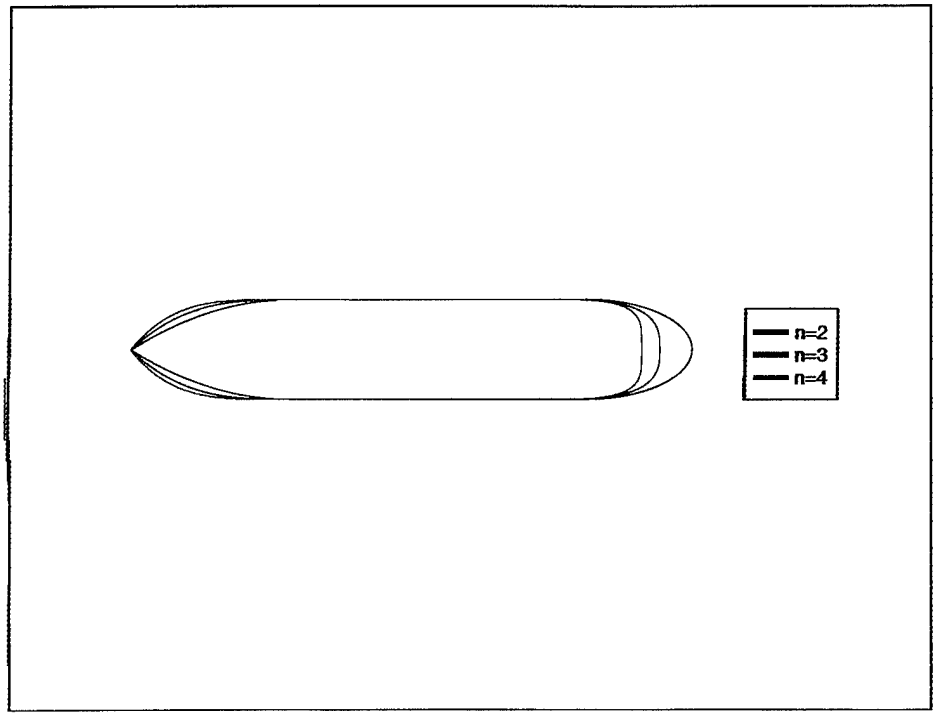

Figure 2. The effect of changing the shape factors for the limited diameter case.

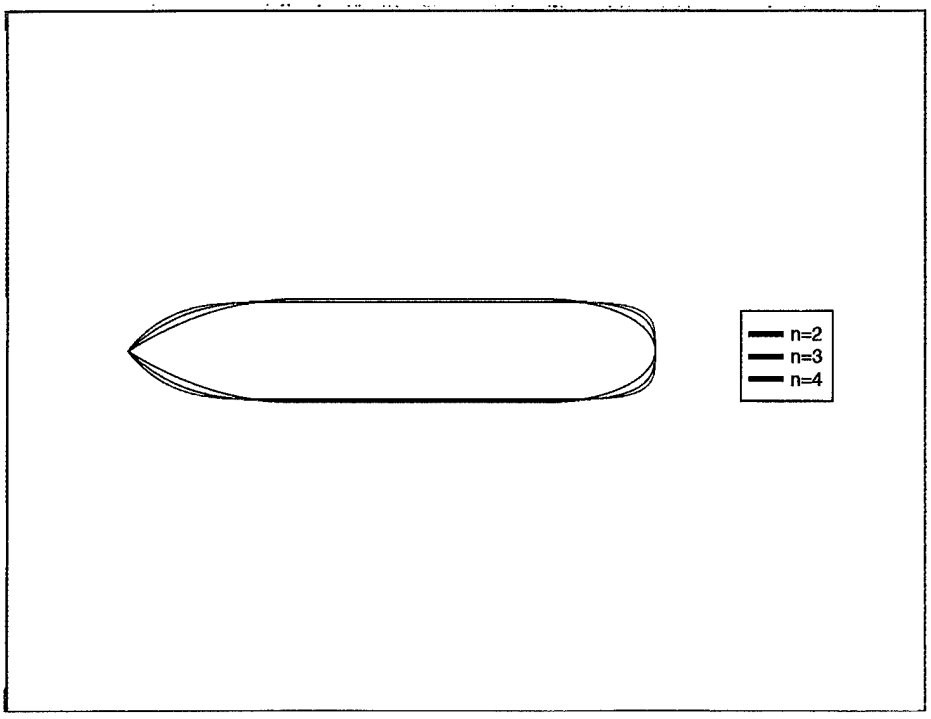

Figure 3. The effect of changing the shape factors for the limited length case.

body the prismatic coefficient can be evaluated in terms of its geometry. Using the above concept, L_{PMB} is the difference between the overall length and six times the diameter, that is *L-6D*. A method of calculating the volume of the entire hull can be developed by calculating the volume of each section separately by using the expressions above. Let V_f, V_a, and V_{PMB} denote volumes of the entrance, the run, and the PMB, respectively. The resulting equations are:

$$V_f = \frac{\pi D^2}{4}\left(C_{pf} 2.4D\right) \tag{3}$$

$$V_a = \frac{\pi D^2}{4}\left(C_{pa} 3.6D\right) \tag{4}$$

$$V_{PMB} = \frac{\pi D^2}{4}\left(L - 6D\right) \tag{5}$$

The above can be combined into the following,

$$V = \frac{\pi D^3}{4}\left[3.6C_{pa} + \frac{L}{D} - 6 + 2.4C_{pf}\right] \tag{6}$$

It can be easily shown that the prismatic coefficients can be calculated as,

$$C_{pf} = \int_0^1 (1 - x^{n_f})^{2/n_f}\, dx \tag{7}$$

$$C_{pa} = \int_0^1 (1 - x^{n_a})^2\, dx \tag{8}$$

These integrals are numerically evaluated using the built in "quad" function in Matlab, although analytic evaluation is possible,

$$C_{pa} = \frac{2n_a^2}{1+3n_a+2n_a^2} \tag{9}$$

$$C_{pf} = \frac{\Gamma\left(1-\frac{2}{n_f}\right)\Gamma\left(\frac{1}{n_f}\right)}{n_f\Gamma\left(1+\frac{33}{n_f}\right)} \tag{10}$$

where the Gamma function is defined in Ref. 4 (Abramowitz and Stegun, 1970).

Initially, the total volume is calculated for the values of L =360 ft., D = 30 ft., n_a = 3.0 and n_f = 3.0, by using Equations (6) through (8), and yielded a value of 217337.73 ft^3. This value is kept constant throughout the calculations.

For the limited length case, L is kept constant at 360 ft. The shape factors n_a and n_f are varied between 2.0, 3.0 and 4.0. The prismatic coefficients C_{pa} and C_{pf} are calculated for each of them by evaluating the integrals in Equations (7) and (8) numerically. Then the corresponding diameters are found by solving for the maximum hull diameter D in Equation (6). This is achieved by solving the following cubic equation,

$$(3.6C_{pa}+2.4C_{pf}-6)D^3+LD^2-\frac{4V}{\pi}=0 \tag{11}$$

Two iterations ensure that the solution converges to the value which meets the requirement to have L_a=3.6D and L_f=2.4D.

For the limited diameter case, D is kept constant at 30 ft. C_{pa} and C_{pf} are calculated the same way as the limited length case. Then the corresponding lengths are found by solving for L in Equation (6).The resulting equation becomes,

$$L = D\left(\frac{4V}{\pi}D^3 - 3.6C_{pa} - 2.4C_{pf} + 6\right) \tag{12}$$

Two Matlab programs (Appendix) are used to perform the calculations for each case. In the limited length case, the program "limlen" starts by inputting n_a and n_f, and computes the corresponding diameter. Similarly, for the limited diameter case, the program "limdia" computes the length for the given n_a and n_f values. These values are used as an input in the strip theory seakeeping prediction program.

B. MOTIONS IN A SEAWAY

Wave patterns in an open sea are ever changing with time and space, in a manner that appears to defy analysis be it linear or second order Stokes [Ref 5]. Ambient waves on the surface of the sea are dispersive as well as random. Random refers to the character of the wave height distribution. In a continuous distribution, the sinusoidal waves have continuously distributed amplitude and phase so that in summation the variation of wave height with time is not systematic in any respect, but random. The generating mechanism is, predominantly, the effect upon the water surface of wind in the atmosphere. The practically useful data extractable from a random wave record $h(t)$ is its spectral density, $S(\omega)$. The random $h(t)$ record is processed in such a way to produce a curve of $S(\omega)$ versus wave frequency, ω. The spectral density is obtained from a wave height record taken over a time period for which the sea conditions are assumed to be unchanging, in an average sense (stationary). This corresponds to a certain sea state. The function $S(\omega,\theta)$ is called the spectral energy density or simply the energy spectrum. More specifically, this is a directional energy spectrum; it can be integrated over all wave directions to give the frequency spectrum.

$$S(\omega) = \int_0^{2\pi} S(\omega,\theta)d\theta \ . \tag{13}$$

Usually in the fields of ocean engineering and naval architecture it is customary to assume that the waves are long crested which means the fluid motion is two dimensional and the wave crests are parallel. With such a simplification it is possible to use existing information for the frequency spectrum (13), which is based on a combination of theory and full scale observations. The sea spectrum (spectral density) gives us information on mean wave height within finite frequency bands. Since most of the wave energy is within a relatively small range of wave lengths where it may resonate the ship, we can model the seaway as a narrow band random process.

For most purposes we are interested primarily in the larger waves. The most common parameter that takes this into account is the significant wave height, $H_{1/3}$, defined as the average of the highest one third of all waves. This is computed by

$$H_{1/3} = 4.0(m_0)^{1/2}. \tag{14}$$

In this equation, m_0 is the area under the spectrum $S(\omega)$ integrated over the entire range of frequencies ω. An average frequency of the spectrum can be defined as the expected number of zero upcrossings per unit time, that is, the number of times the wave amplitude passes through zero with positive slope. The final result here is

$$\omega_z = \left(\frac{m_2}{m_0}\right)^{1/2}. \tag{15}$$

The average period between zero upcrossings is

$$T_z = \frac{2\pi}{\omega_z} = 2\pi\sqrt{\frac{m_0}{m_2}} \tag{16}$$

More meaningful frequency parameters can be obtained from the set of moments, which depend on spectrum shape

$$m_n = \int_0^\infty \omega^n S(\omega) d\omega \ , \qquad n=0,1,2,... \tag{17}$$

In particular, the area, m_0, is the variance or the total energy of the spectrum. Also m_2 is variance of velocity and m_4 is variance of acceleration.

A good model for fully developed seas is the classical Pierson-Moskowitz spectrum. This spectral form depends upon a single parameter which is the significant wave height. It is intended to represent point spectrum of a fully-developed sea. Fetch and duration are assumed to sufficiently large so that the sea has reached steady state, in a statistical sense. This spectral family should be recognized as an asymptotic form, reached after an extended period of steady wind, with no contamination from an underlying swell. Using the spectral family, along with the similarity theory of S. A. Kitaigorodskii, Pierson and Moskowitz (1964) [Ref. 5] arrived at the following analytical formulation for ideal sea spectra,

$$S_1^+(\omega) = \frac{0.0081 g^2}{\omega^5} \exp\left[-0.032\left(\frac{g}{H_{1/3}\omega^2}\right)^2\right], \tag{18}$$

where

$S_1^+(\omega)$ = one-sided incident wave spectrum

g = acceleration of gravity

$H_{1/3}$ = significant wave height

ω = wave frequency

In Figure 4 we can observe typical Pierson-Moskowitz wave spectra for 5 m. significant wave height.

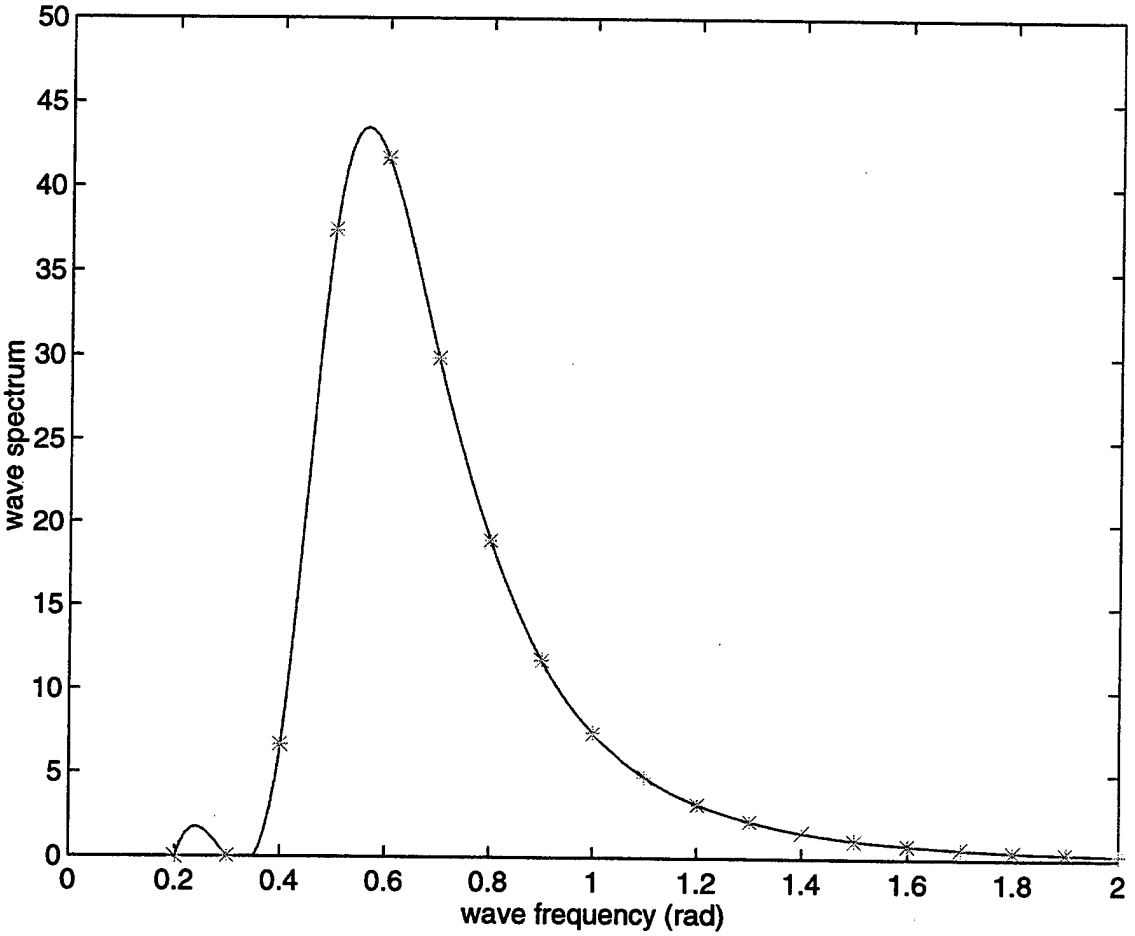

Figure 4. Typical Pierson-Moskowitz wave spectra

Any conclusions drawn on the seakeeping behavior of a ship based on the critical examination of motion response in regular waves can, at best, assume only academic significance. The establishment of the seakeeping behavior of a ship has to be done in a realistic seaway. With the spectral description of sea waves given before, we can return to the subject of body motions and generalize the results of regular harmonic waves. If the sea waves are described by the random distribution , and if the response of the body to

each component wave is defined by a response amplitude operator $Z(\omega,\theta)$, the body response will be

$$\eta_j(t) = \Re\iint Z_j(\omega,\theta)e^{i\omega t}dA(\omega,\theta) \ . \qquad \textbf{(19)}$$

The principal assumption here is that linear superposition applies, as it must in any event for the underlying development of the RAO and the spectrum.

Like the waves themselves, the response (19) is a random variable. The statistic of the body response are identical to the wave statistics, except that the wave energy spectrum S is multiplied by the square of the RAO (this is a property of linear systems). Thus, if the subscript R represents any body response, we have

$$S_R(\omega) = |Z_R(\omega)|^2 S(\omega) \ , \qquad \textbf{(20)}$$

where $Z_R(\omega)$ is the RAO of the response R, and $S(\omega)$ the spectrum of the seaway. Equation (20) can then be utilized to obtain the spectrum of the response R. Figure 5 displays the spectrum of response of the relative vertical motion at the top of our model submarine's sail while submarine's forward speed is 5 Knots and it is at 3 submarine diameter depth. Also seaway is modeled by Pierson-Moskowitz spectrum with 5 m. significant wave height and head seas.

To a large extent, equation (20) provides the justification for studying regular wave responses. The transfer function $Z_R(\omega)$ is valid not only in regular waves, where it has been derived, but also in a superposition of regular waves, and ultimately in a spectrum of random waves. Generally speaking, a vessel with favorable response characteristics in regular waves will be good in irregular waves, and vice versa.

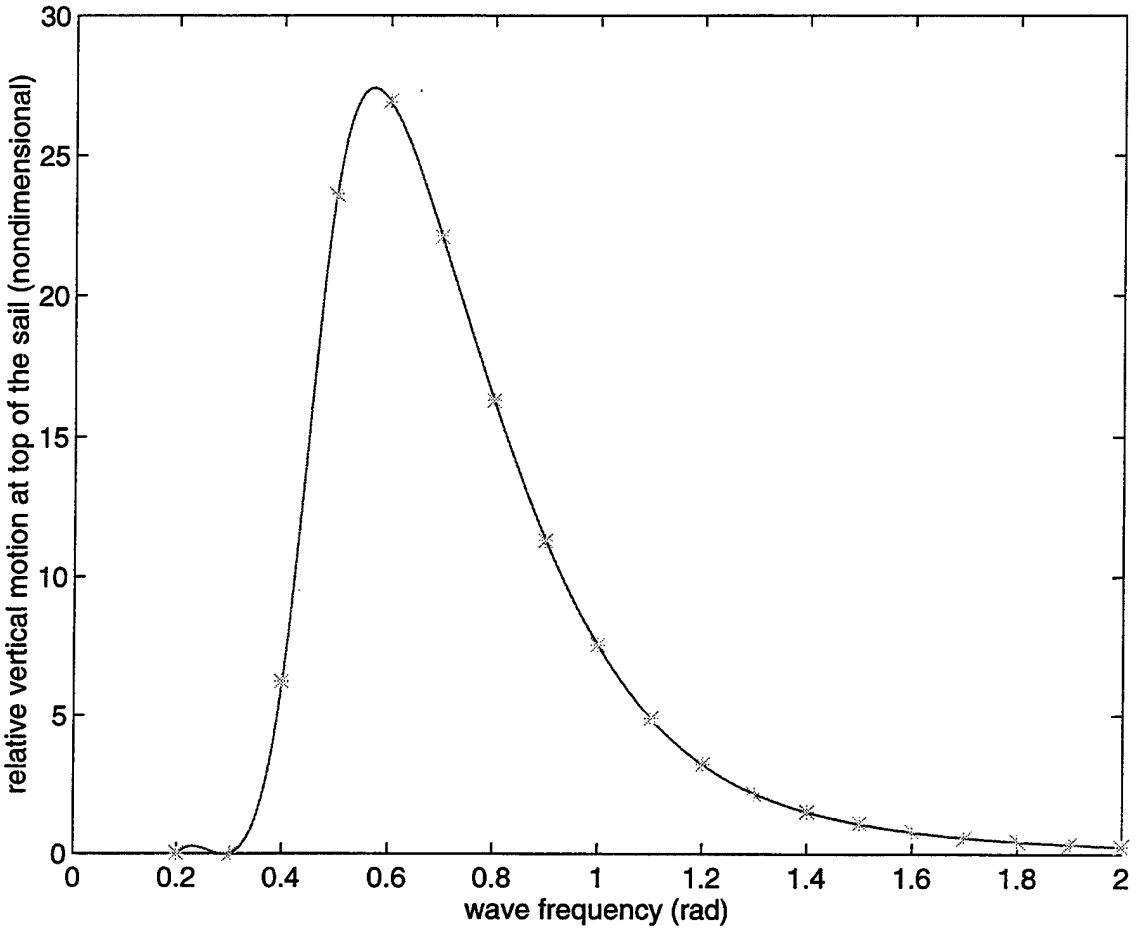

Figure 5. Spectrum of response for relative vertical motion.

The average period between zero upcrossings was determined by Equation (16), and the number between zero upcrossings per unit time is

$$N_z^R = \frac{1}{2\pi}\sqrt{\frac{m_2^R}{m_0^R}}\ , \tag{21}$$

where m_0^R, m_2^R are the moments of the particular response R, whose spectral density is given by Equation (20). Equation (21) can be generalized for the case of the average number of upcrossings above a specified level α as in

$$N_{z,\alpha}^R = \frac{1}{2\pi}\sqrt{\frac{m_2^R}{m_0^R}}\exp\left(-\frac{\alpha^2}{2m_0^R}\right). \tag{22}$$

Equation (22) can be utilized to determine such events deck wetness and bow slamming for a surface ship or periscope submergence and sail broaching for a near surface submarine. If f represents height of the periscope over calm sea surface level, the number of periscope submergence events per hour is

$$N_p = 3600\frac{1}{2\pi}\sqrt{\frac{m_2}{m_0}}\exp\left(-\frac{f^2}{2m_0}\right), \tag{23}$$

where m_0 , m_2 are the moments of the vertical relative motion spectrum at periscope. The same equation can be used to estimate the frequency of sail broaching, with f substituted by the distance between top of the sail and encountered wave surface. Of course, m_0 , m_2 are now the moments of the relative motion spectrum at top of the sail.

III. RESULTS

A. OPERABILITY INDEX

In this study two criteria are considered for the near surface operations of the submarine in deep water, for both the limited diameter and the limited length cases. First is the number of periscope submergence events per hour (N_{p1}), which can be calculated using Equation (23) and selected as 300, which corresponds to five periscope submergence events per minute. This is an arbitrary number and different numbers could be picked for different operational considerations. The same number is used for all cases to represent all possible choices. The other criterion is the number of sail broaching events per hour (N_{p2}), which can be also calculated from Equation (23) and selected as one. Since a single event occurrence may result in submarine detection, this places far greater emphasis on sail broaching than periscope submergence.

Having the tools to compute the two performance indices defined above in a given seaway. Suppose that the submarine conducts periscope depth operation in a seaway characterized by a significant wave height (Pierson-Moskowitz Wave Spectrum), so that the sea spectrum is defined. For all round the clock boat headings relative to the predominant wave direction for which the operations are to be conducted, a polar plot diagram similar to the one in Figure 6 is prepared. Significant wave heights are represented along the radial direction of the polar plot. The shaded area in the plot shows wave height and wave direction combinations where the selected tactical assessment criterion is exceeded. Three plots are combined on a single plot for different shape factors, which are selected as two, three and four at the same speed/depth combination. Letting

the polar area of the disk in Figure 6 be A_o and the subset of A_o within which the boat can conduct the operation be A, a performance index characterizing the ability of the boat perform this operation in the specified submarine velocity and depth can be defined as $100(A/A_o)$. Generally a submarine's forward speed ranges from three to twelve knots in periscope depth operations. We used three, five, eight and eleven knots submarine forward speeds, U, in our calculations. Depths, h, beneath the surface were selected from 1.5 to 2.5 boat diameters measured from the keel up. The calculations are repeated for both the limited diameter and the limited length cases and for the shape factors n_a *and* n_f, which are selected as two, three and four. In computing the above index we could easily take into account the probability of occurrence of a particular sea state and wave heading angle in the area of interest by introducing appropriate weight factors. In this study we assumed that all possible sea-states and wave heading angles are equally probable. In the following sections we discuss the results for both criteria/operability indexes and also for the combined criterion/operability index, where both criteria are taken into consideration at the same time. In each case, combined plots for different shape factors at certain speed/depth combination are shown.

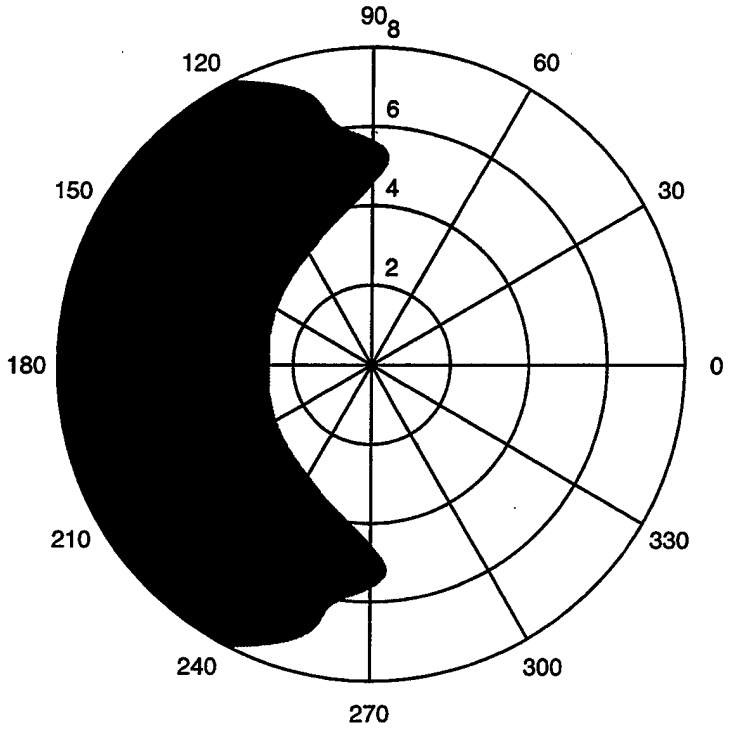

Figure 6. Typical performance assessment of a submarine.

B. PERISCOPE SUBMERGENCE CRITERION RESULTS

The operability indices for the periscope submergence criterion for the limited diameter and limited length cases in different speeds, operating depths and shape factors are shown in Tables I and II, and in Figure 7. Typical polar plots are shown in Figures 8 through 30. Based on these results, the following conclusions can be drawn:

1. Regardless of the variation of the parameters in the criterion, head seas appear to result in a larger number of expected criterion violations than following seas. This is valid for both limited length and limited diameter cases.

2. Changes in the shape factors appear to have greater effects at smaller speeds and larger operating depths. At smaller depths, smaller shape factors yield slightly higher operability indices, while at larger depths and larger speeds, the reverse may occur.

3. An optimum shape factor for a certain operating depth, which minimizes the expected number of periscope submergence events can be found, and this appears to be a weak function of speed.

4. Similar values of the operability index may result in very different response characteristics. This is because the shape shape of the polar plots may be quite different, even though their areas are the same.

		LIMITED DIAMETER			
		U=3	U=5	U=8	U=11
h=1.5D	n=2	0.7228	0.6614	0.6270	0.6154
	n=3	0.6244	0.6102	0.5974	0.5903
	n=4	0.6192	0.6080	0.5935	0.5840
h=2D	n=2	0.7145	0.7351	0.6239	0.6053
	n=3	0.6772	0.6332	0.6163	0.5898
	n=4	0.6003	0.5914	0.5823	0.5806
h=2.5D	n=2	0.7050	0.6309	0.5941	0.6109
	n=3	0.6382	0.6313	0.6947	0.6165
	n=4	0.6897	0.7379	0.6578	0.6035

Table I : Operability indices for periscope submergence criterion for the limited diameter case.

		LIMITED LENGTH			
		U=3	U=5	U=8	U=11
h=1.5D	n=2	0.6313	0.6153	0.6027	0.6037
	n=3	0.6244	0.6102	0.5974	0.5903
	n=4	0.6264	0.6102	0.5955	0.5897
h=2D	n=2	0.7717	0.7268	0.6320	0.6219
	n=3	0.6772	0.6332	0.6163	0.5898
	n=4	0.6266	0.6102	0.5973	0.6009
h=2.5D	n=2	0.7703	0.6640	0.6097	0.5852
	n=3	0.6382	0.6313	0.6947	0.6165
	n=4	0.6863	0.7349	0.6513	0.6037

Table II : Operability indices for periscope submergence criterion for the limited length case.

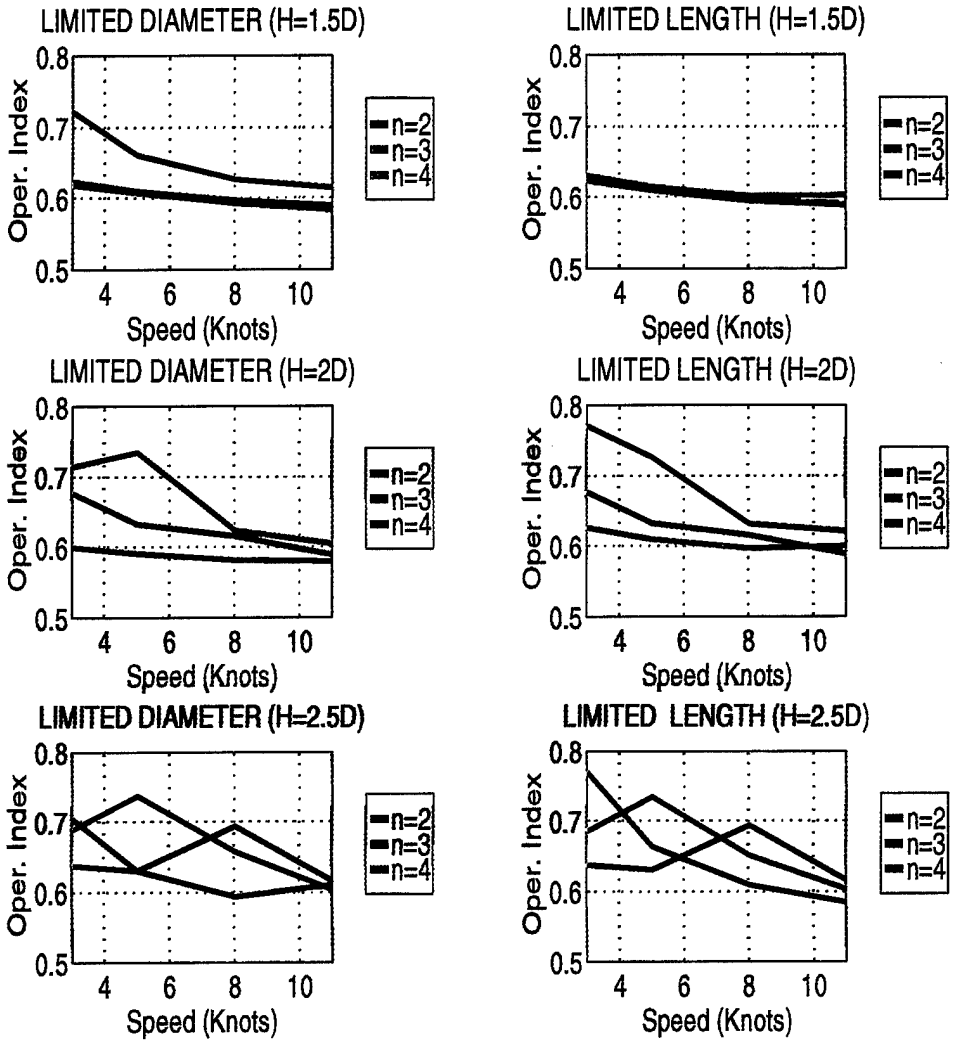

Figure 7. OI vs. submarine speed plots for periscope submergence criterion.

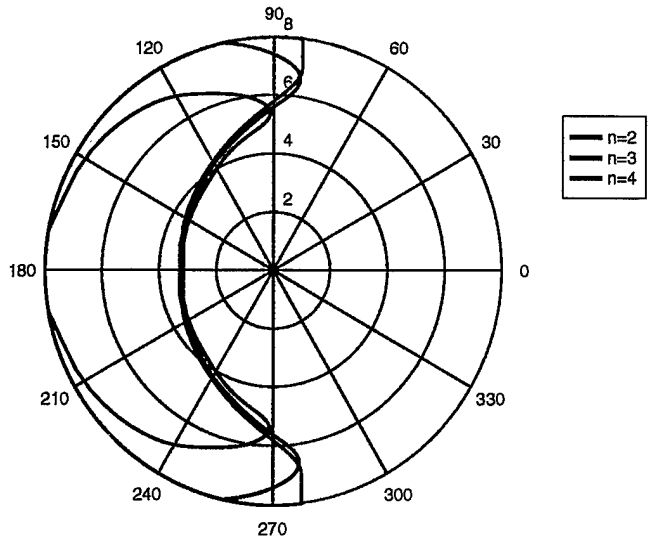

Figure 8. Sea state-polar plot, showing the effect of shape factors in limited diameter case, for U=3 Knots, h=1.5D.

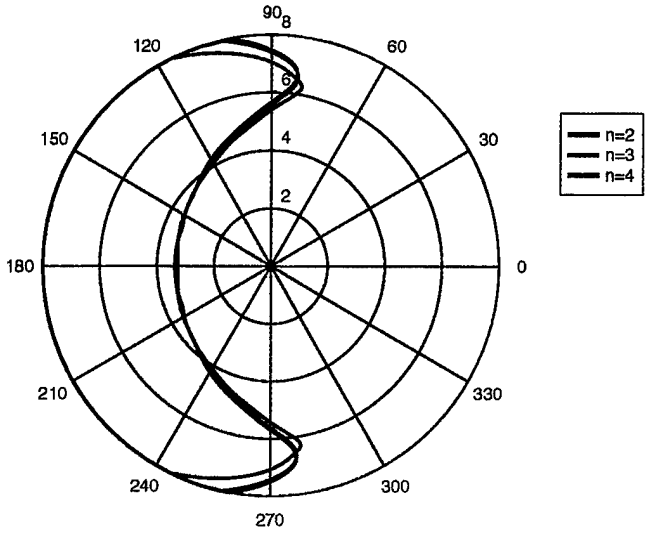

Figure 9. Sea state-polar plot, showing the effect of shape factors in limited length case, for U=3 Knots, h=1.5D.

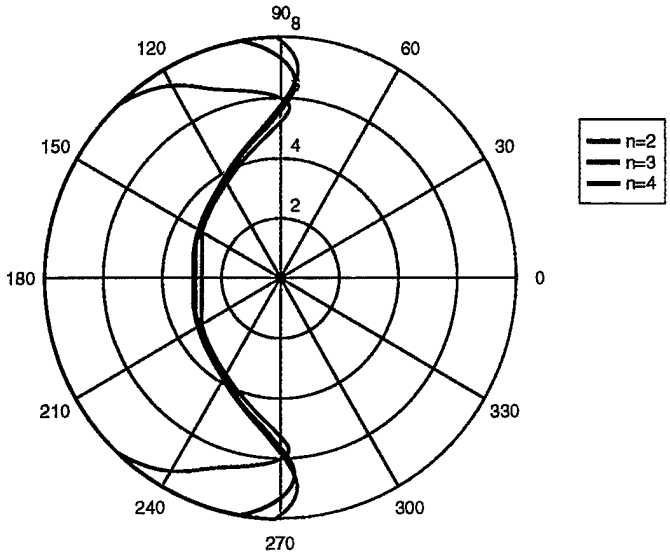

Figure 10. Sea state-polar plot, showing the effect of shape factors in limited diameter case, for U=5 Knots, h=1.5*D*.

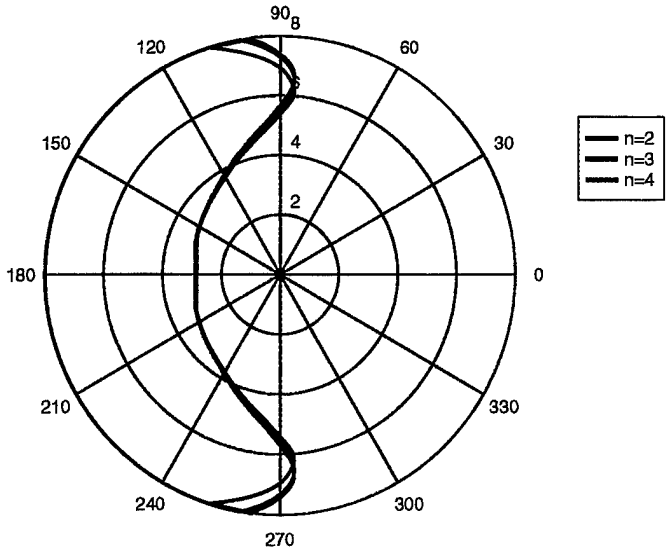

Figure 11. Sea state-polar plot, showing the effect of shape factors in limited length case, for U=5 Knots, h=1.5*D*.

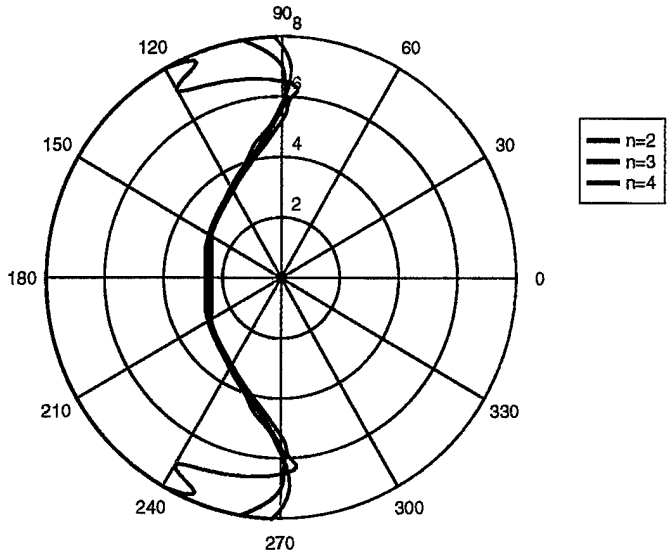

Figure 12. Sea state-polar plot, showing the effect of shape factors in limited diameter case, for U=8 Knots, h=1.5*D*.

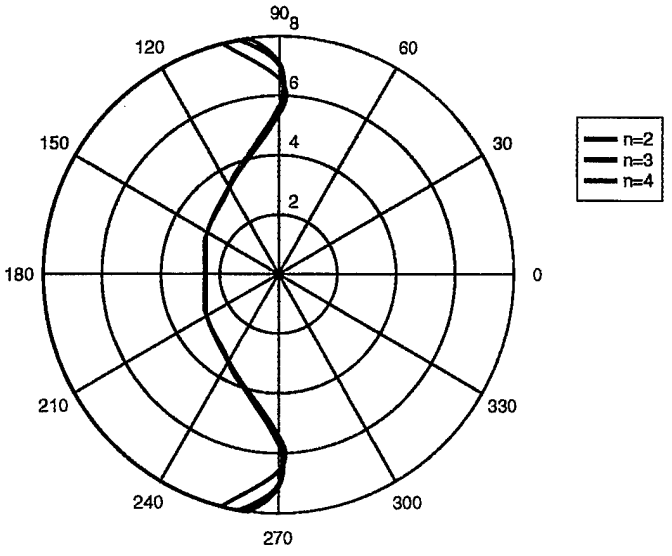

Figure 13. Sea state-polar plot, showing the effect of shape factors in limited length case, for U=8 Knots, h=1.5*D*.

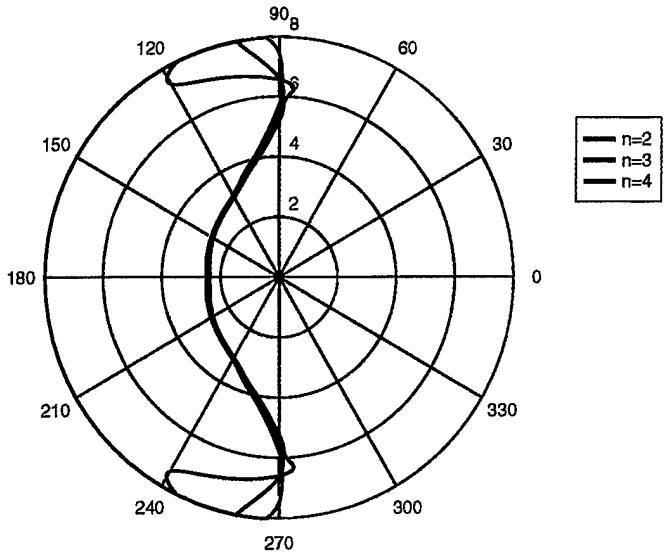

Figure 14. Sea state-polar plot, showing the effect of shape factors in limited diameter case, for U=11 Knots, h=1.5*D*.

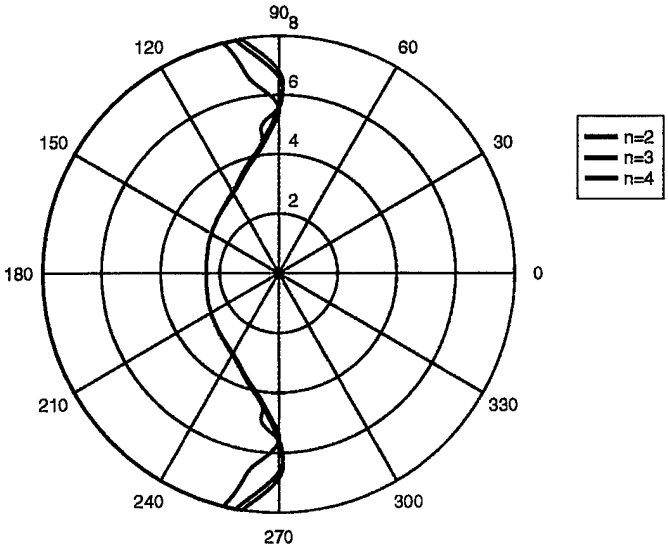

Figure 15. Sea state-polar plot, showing the effect of shape factors in limited length case, for U=11 Knots, 1.5*D*.

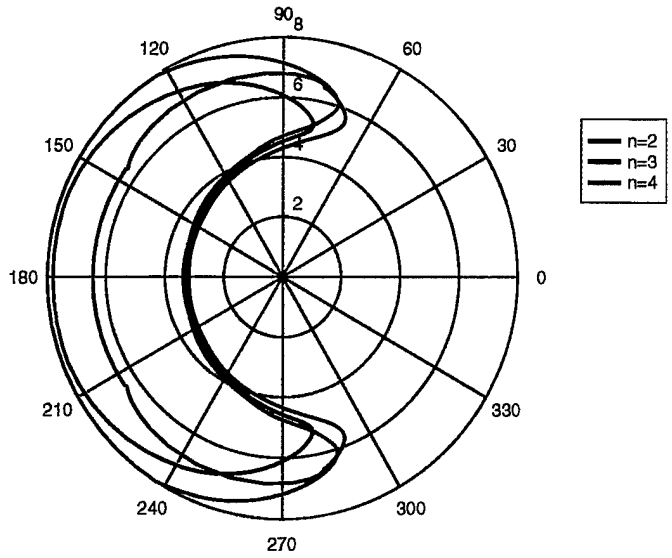

Figure 16. Sea state-polar plot, showing the effect of shape factors in limited diameter case, for U=3 Knots, h=2*D*.

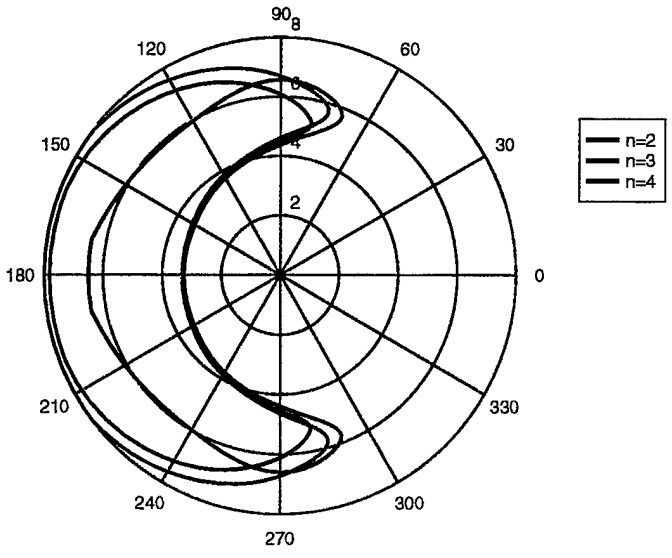

Figure 17. Sea state-polar plot, showing the effect of shape factors in limited length case, for U=3 Knots, h=2*D*.

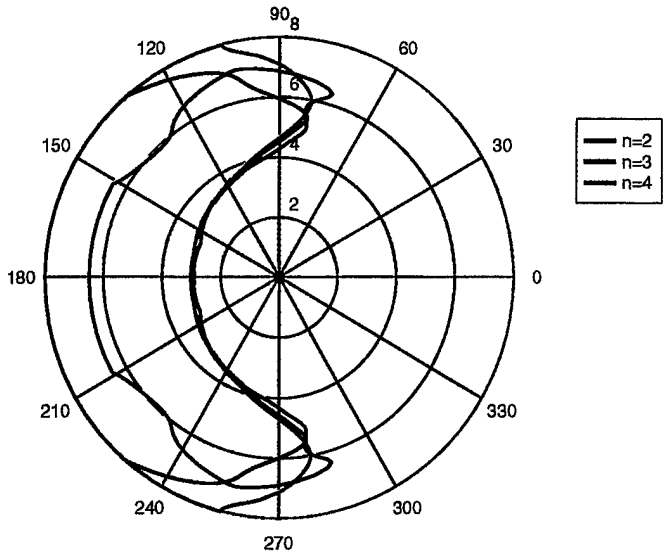

Figure 18. Sea state-polar plot, showing the effect of shape factors in limited diameter case, for U=5 Knots, h=2*D*.

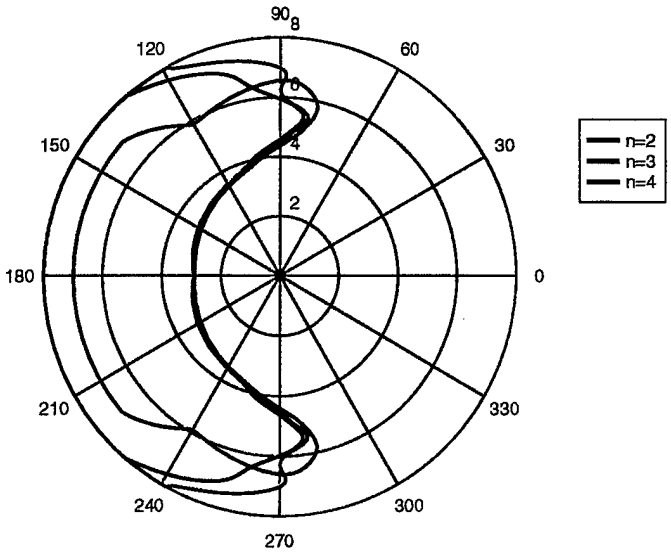

Figure 19. Sea state-polar plot, showing the effect of shape factors in limited length case, for U=5 Knots, h=2*D*.

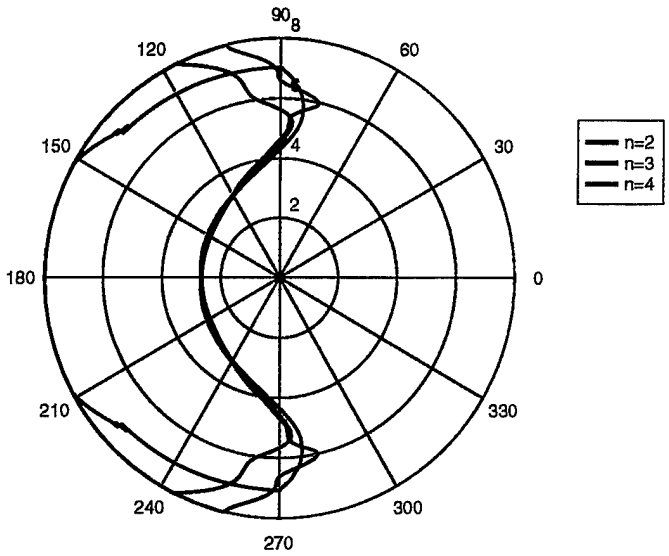

Figure 20. Sea state-polar plot, showing the effect of shape factors in limited diameter case, for U=8 Knots, h=2*D*.

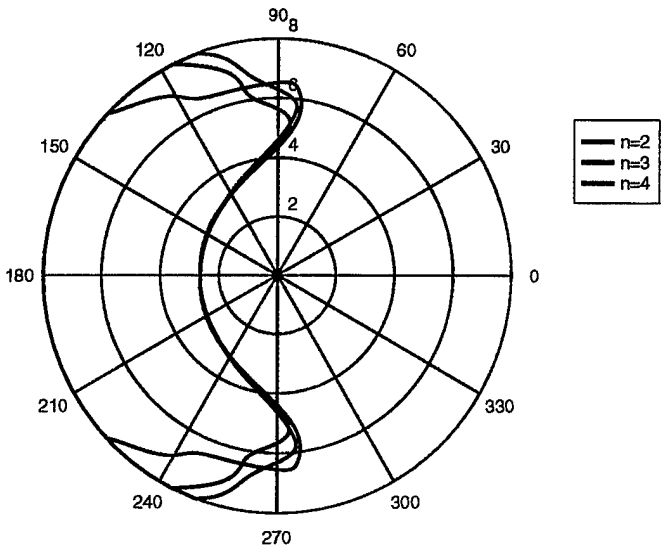

Figure 21. Sea state-polar plot, showing the effect of shape factors in limited length case, for U=8 Knots, h=2*D*.

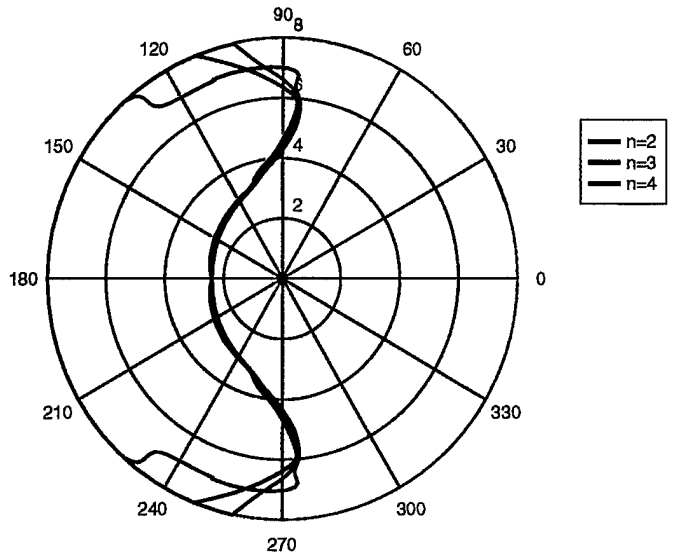

Figure 22. Sea state-polar plot, showing the effect of shape factors in limited diameter case, for U=11 Knots, h=2*D*.

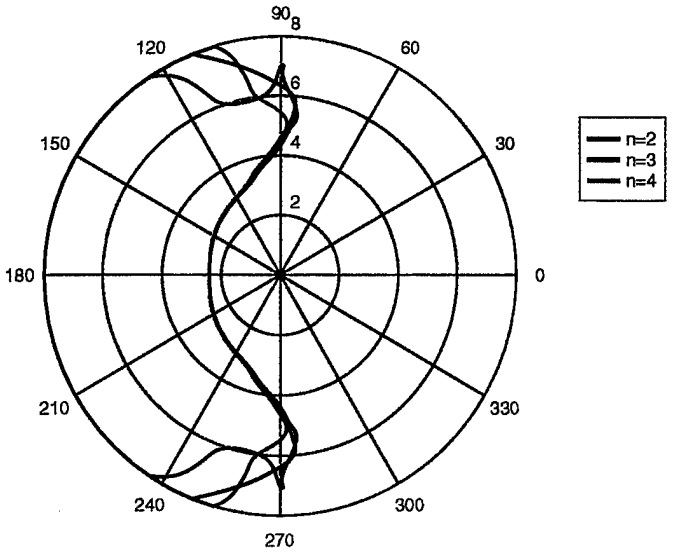

Figure 23. Sea state-polar plot, showing the effect of shape factors in limited length case, for U=11 Knots, h=2*D*.

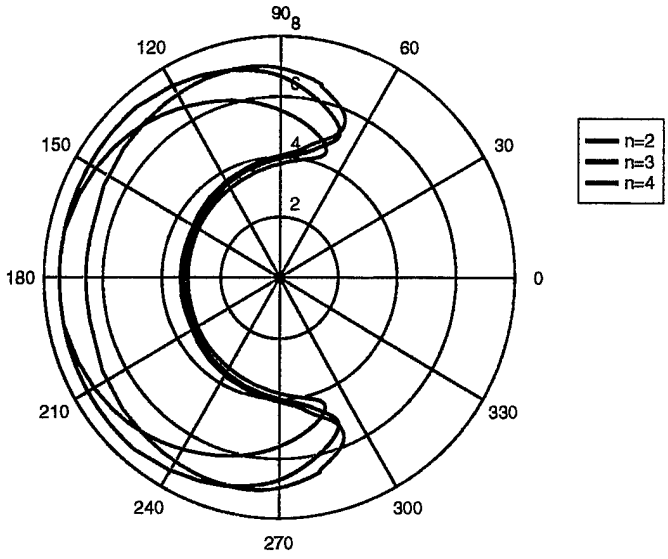

Figure 24. Sea state-polar plot, showing the effect of shape factors in limited diameter case, for U=3 Knots, h=2.5*D*.

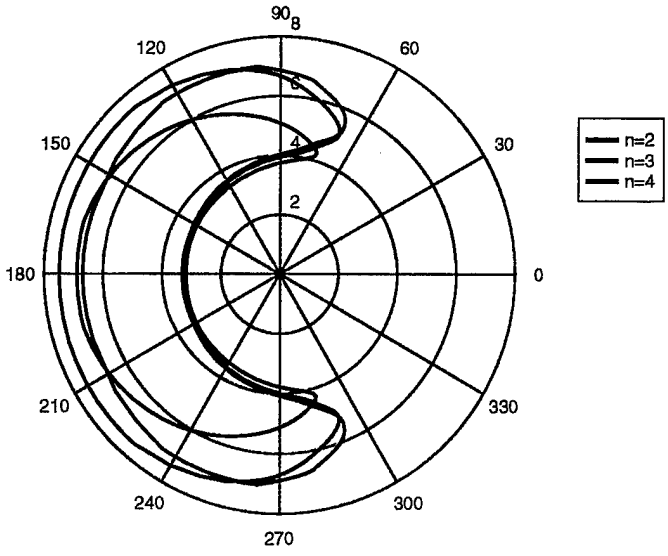

Figure 25. Sea state-polar plot, showing the effect of shape factors in limited length case, for U=3 Knots, h=2.5*D*.

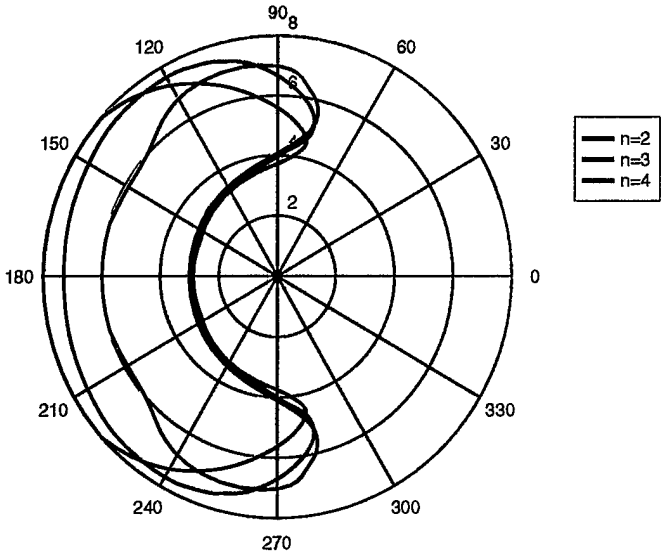

Figure 26. Sea state-polar plot, showing the effect of shape factors in limited diameter case, for U=5 Knots, h=2.5*D*.

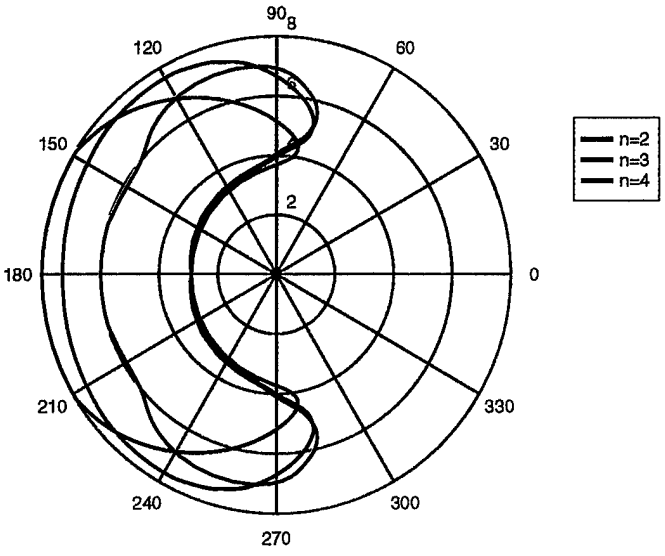

Figure 27. Sea state-polar plot, showing the effect of shape factors in limited length case, for U=5 Knots, h=2.5*D*.

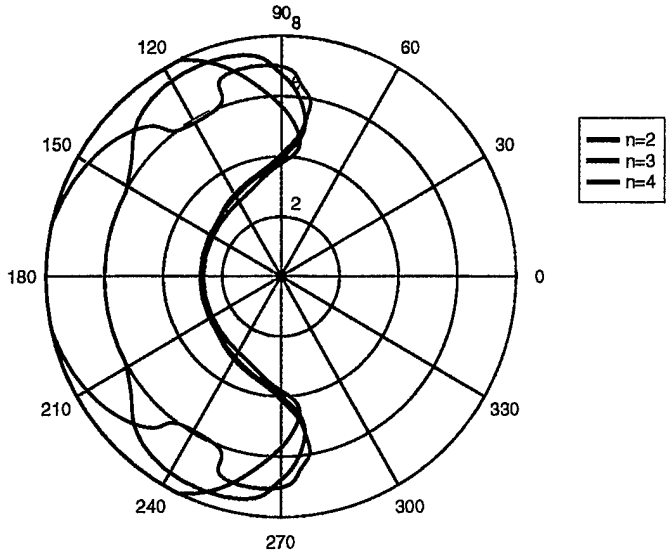

Figure 28. Sea state-polar plot, showing the effect of shape factors in limited diameter case, for U=8 Knots, h=2.5*D*.

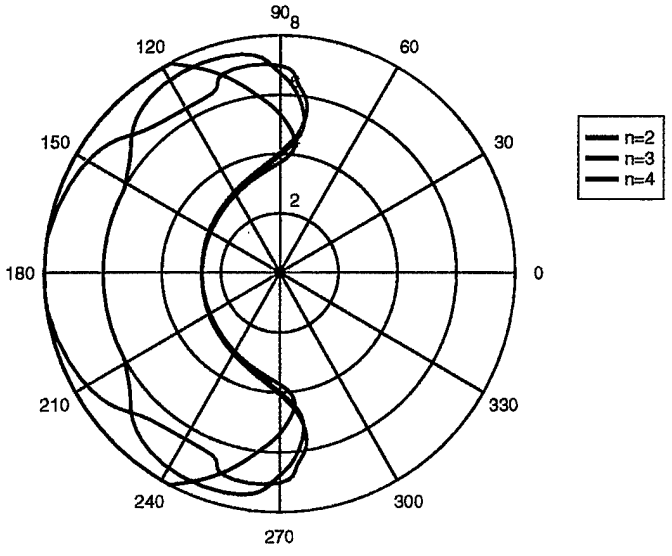

Figure 29. Sea state-polar plot, showing the effect of shape factors in limited length case, for U=8 Knots, h=2.5*D*.

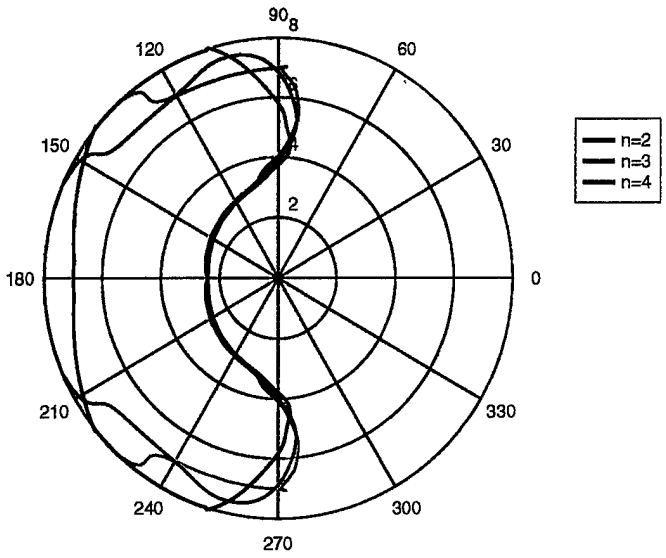

Figure 30. Sea state-polar plot, showing the effect of shape factors in limited diameter case, for U=11 Knots, h=2.5*D*.

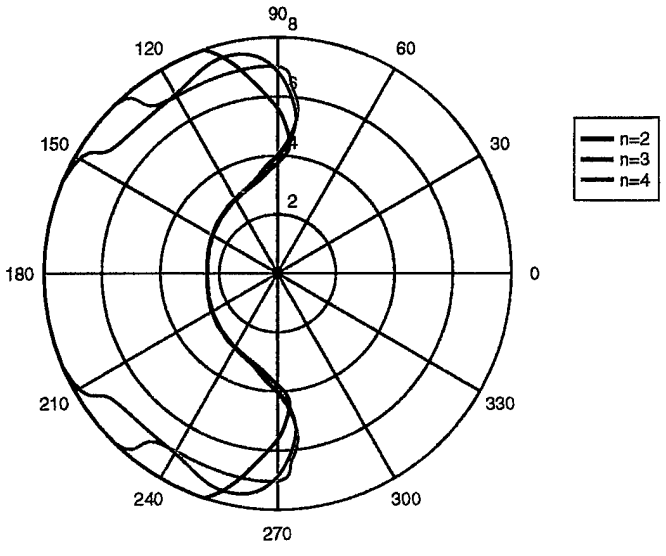

Figure 31. Sea state-polar plot, showing the effect of shape factors in limited length case, for U=11 Knots, h=2.5*D*.

C. SAIL BROACHING CRITERION RESULTS

The operability indices for the sail broaching criterion for the limited diameter and limited length cases in different speeds, operating depths and shape factors are shown in Tables III and IV, and in Figure 32. Typical polar plots are shown in Figures 33 through 56. Based on these results, the following conclusions can be drawn:

1. At smaller speeds, higher shape factors appear to result in smaller number of expected criterion violations. Smaller shape factors generally yield smaller indices.

2. The operability index tends to increase with increasing depth, and in general, it is a weak function of speed for all shape factors.

3. The operability index does not appear to depend on sea direction consistently. At certain directions, the operability index decreases significantly for various shape factor and speed/depth combinations.

		LIMITED DIAMETER			
		U=3	U=5	U=8	U=11
h=1.5D	n=2	0.6101	0.6355	0.7321	0.5423
	n=3	0.7123	0.7138	0.7432	0.7013
	n=4	0.8405	0.8098	0.8029	0.7388
h=2D	n=2	0.9091	0.8768	0.8969	0.7627
	n=3	0.9135	0.9698	0.9635	0.9061
	n=4	0.9235	0.9356	0.9333	0.9816
h=2.5D	n=2	0.8466	0.7435	0.8083	0.7007
	n=3	1.0000	1.0000	0.7813	0.8746
	n=4	0.9777	0.8661	0.9421	0.8258

Table III : Operability indices for the sail broaching criterion for the limited diameter case.

		LIMITED LENGTH			
		U=3	U=5	U=8	U=11
h=1.5D	n=2	0.6173	0.6726	0.6942	0.6070
	n=3	0.7123	0.7138	0.7432	0.7013
	n=4	0.7221	0.7314	0.7452	0.7717
h=2D	n=2	0.8744	0.9005	0.9006	0.8634
	n=3	0.9135	0.9698	0.9635	0.9061
	n=4	0.9068	0.9333	0.9608	0.9479
h=2.5D	n=2	0.6925	0.6920	0.7799	0.7395
	n=3	1.0000	1.0000	0.7813	0.8746
	n=4	0.9761	0.8963	0.9408	0.8310

Table IV : Operability indices for sail broaching criterion for the limited length case.

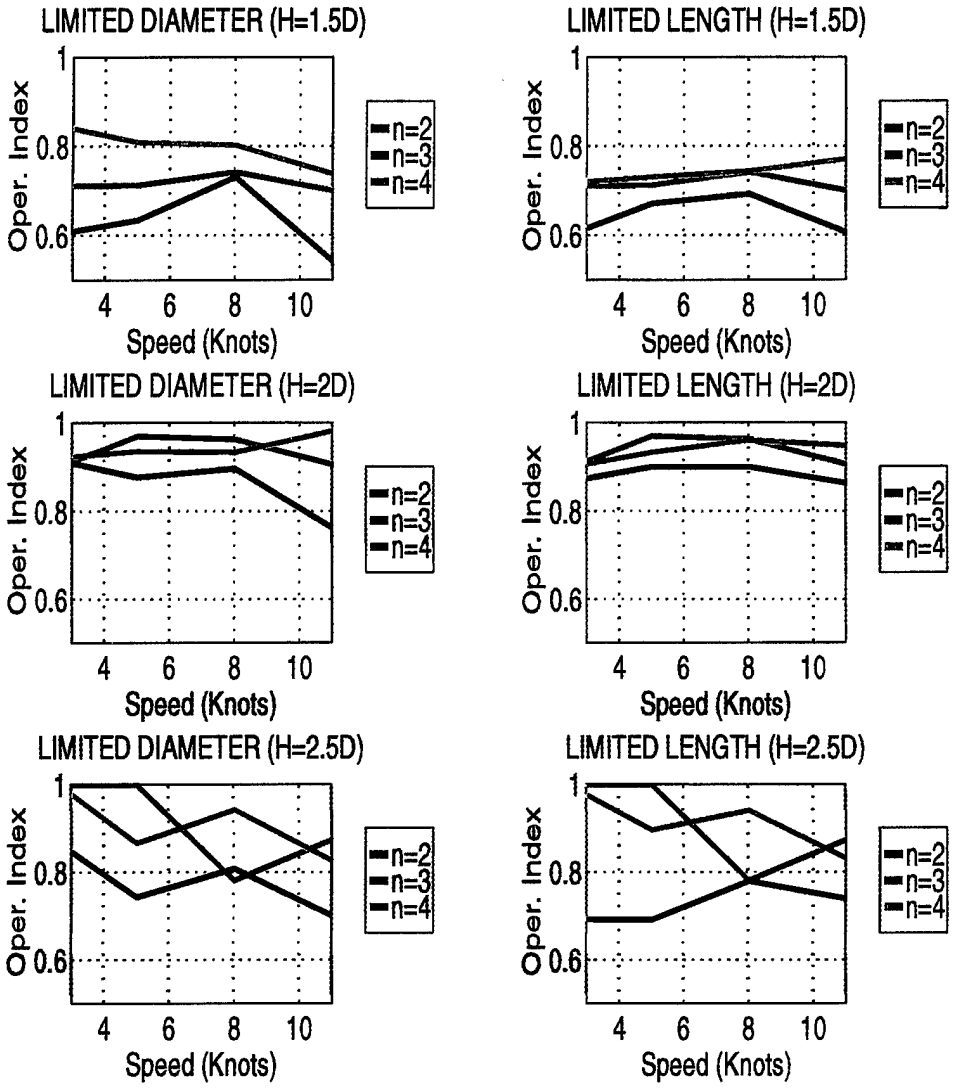

Figure 32. OI vs. submarine speed plots for sail broaching criterion.

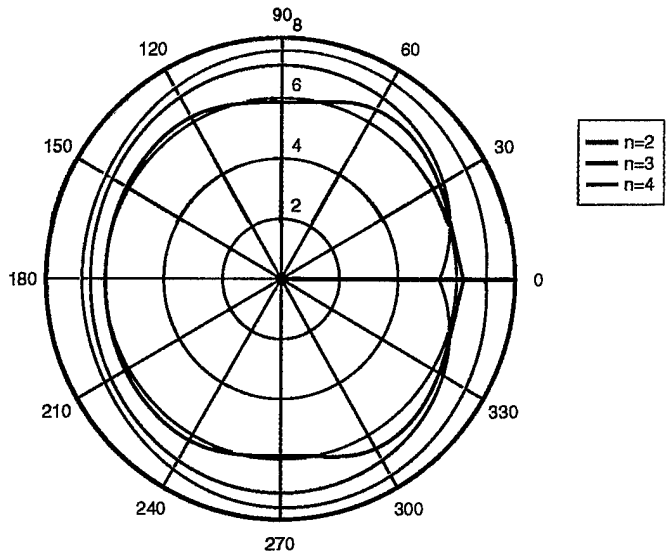

Figure 33. Sea state-polar plot, showing the effect of shape factors in limited diameter case, for U=3 Knots, h=1.5*D*.

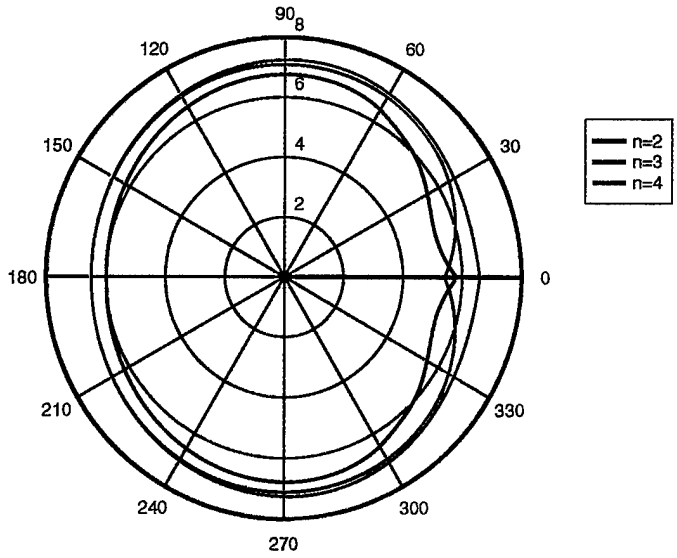

Figure 34. Sea state-polar plot, showing the effect of shape factors in limited length case, for U=3 Knots, h=1.5*D*.

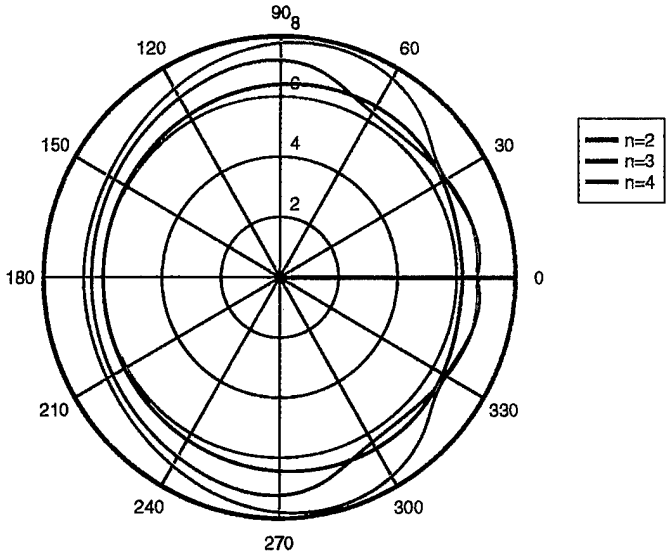

Figure 35. Sea state-polar plot, showing the effect of shape factors in limited diameter case, for U=5 Knots, h=1.5*D*.

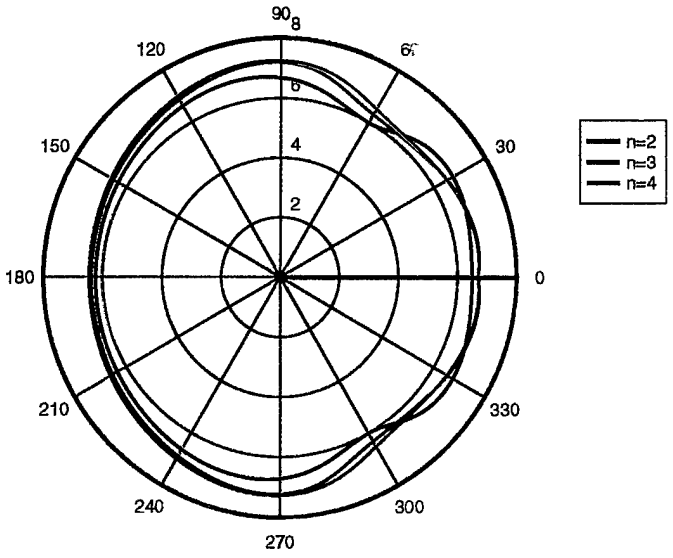

Figure 36. Sea state-polar plot, showing the effect of shape factors in limited length case, for U=5 Knots, h=1.5*D*.

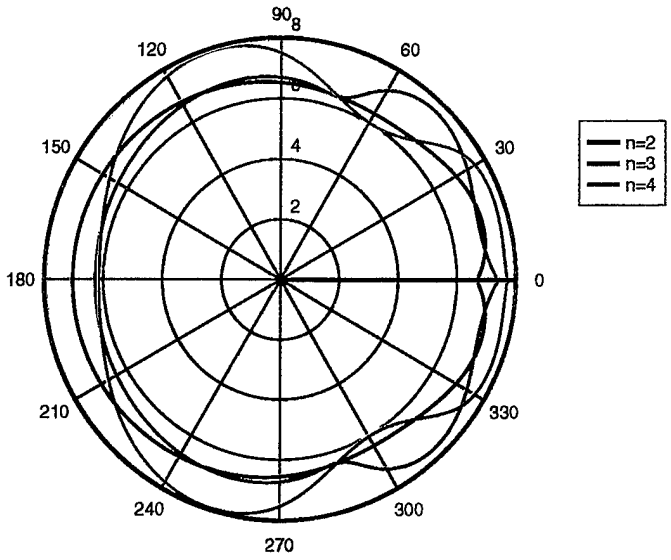

Figure 37. Sea state-polar plot, showing the effect of shape factors in limited diameter case, for U=8 Knots, h=1.5*D*.

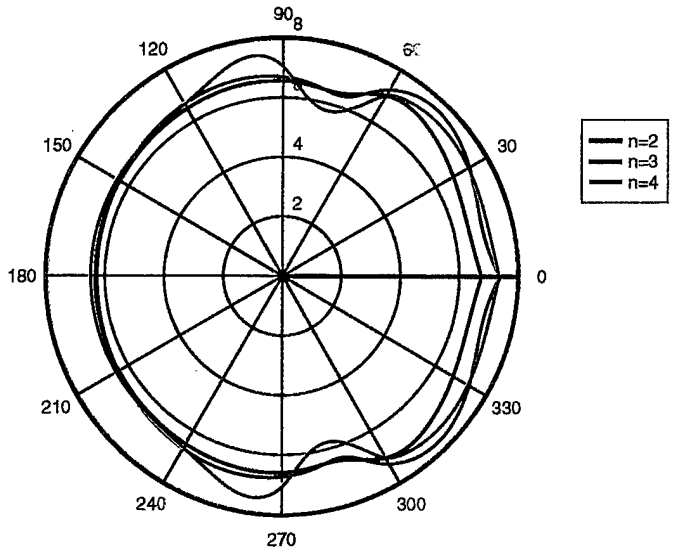

Figure 38. Sea state-polar plot, showing the effect of shape factors in limited length case, for U=8 Knots, h=1.5*D*.

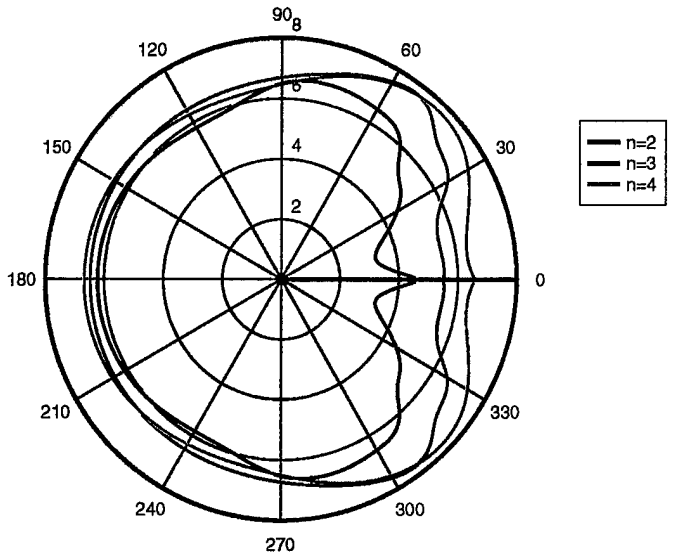

Figure 39. Sea state-polar plot, showing the effect of shape factors in limited diameter case, for U=11 Knots, h=1.5*D*.

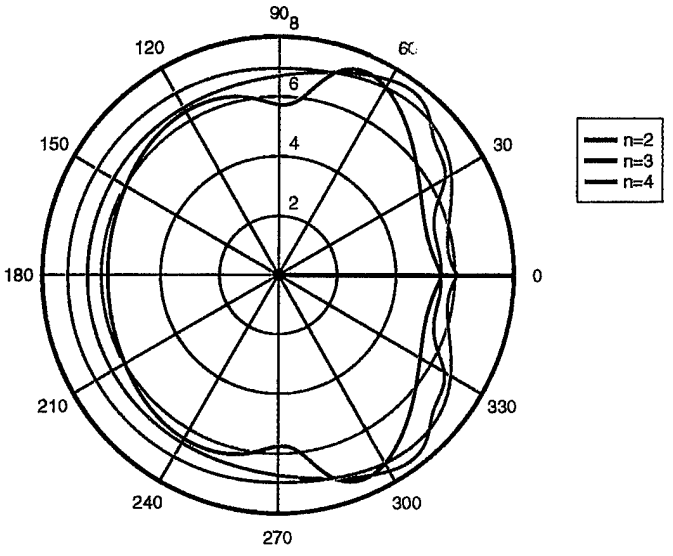

Figure 40. Sea state-polar plot, showing the effect of shape factors in limited length case, for U=11 Knots, h=1.5*D*.

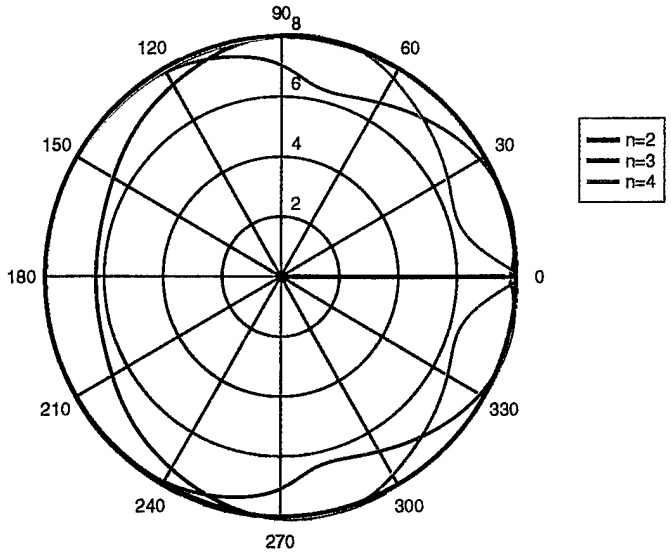

Figure 41. Sea state-polar plot, showing the effect of shape factors in limited diameter case, for U=3 Knots, h=2*D*.

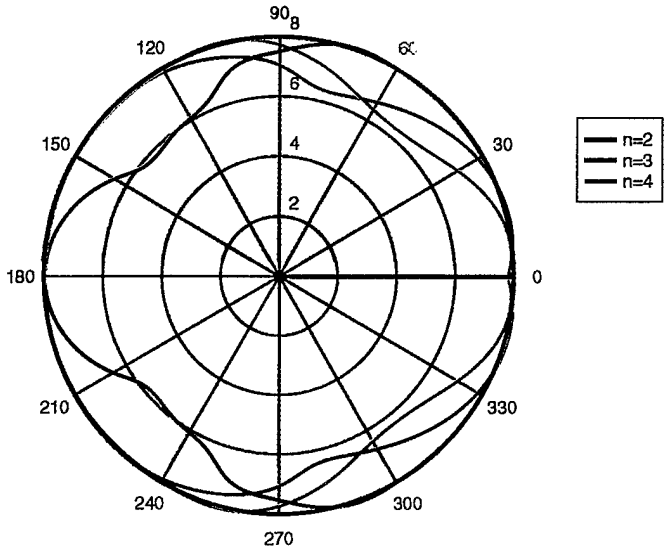

Figure 42. Sea state-polar plot, showing the effect of shape factors in limited length case, for U=3 Knots, h=2*D*.

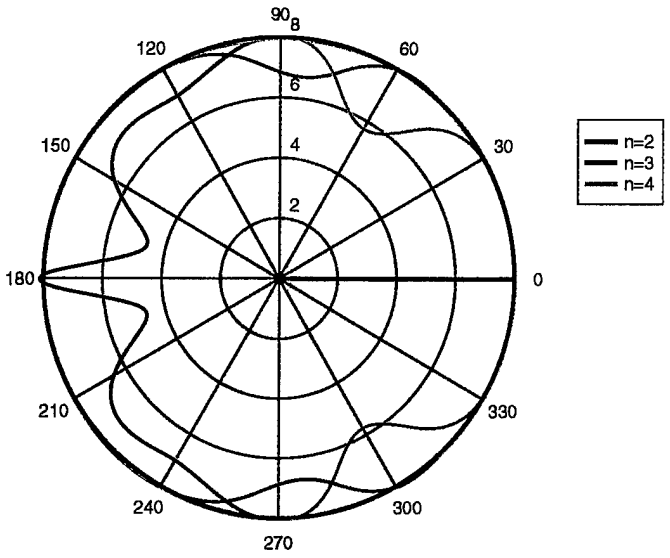

Figure 43. Sea state-polar plot, showing the effect of shape factors in limited diameter case, for U=5 Knots, h=2*D*.

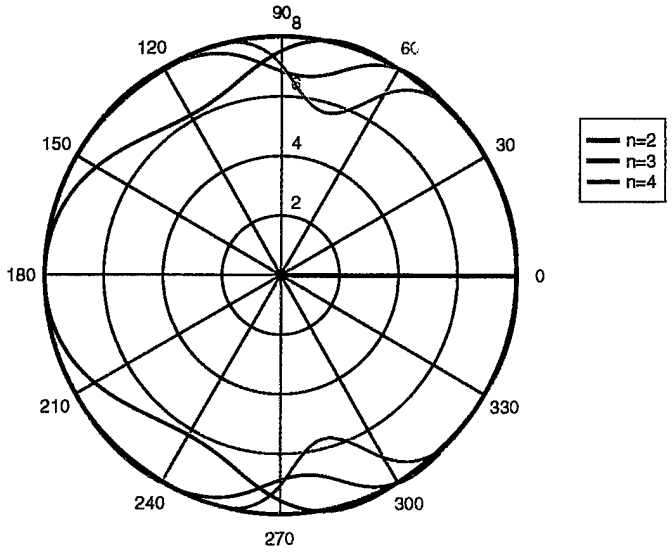

Figure 44. Sea state-polar plot, showing the effect of shape factors in limited length case, for U=5 Knots, h=2*D*.

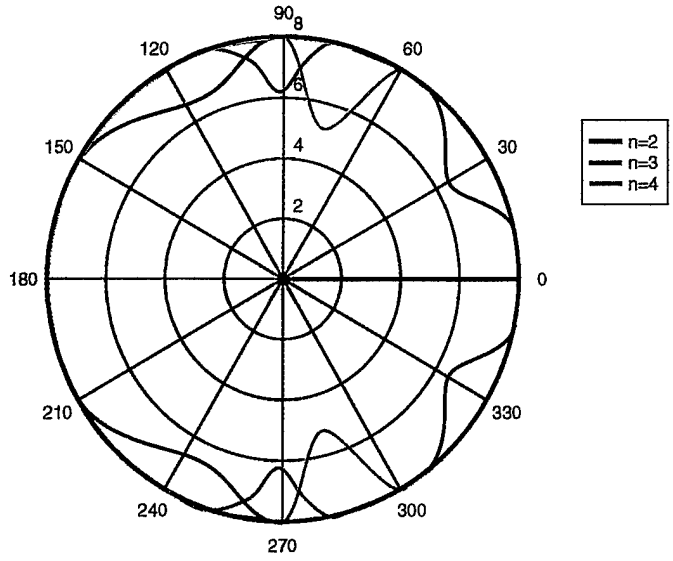

Figure 45. Sea state-polar plot, showing the effect of shape factors in limited diameter case, for U=8 Knots, h=2*D*.

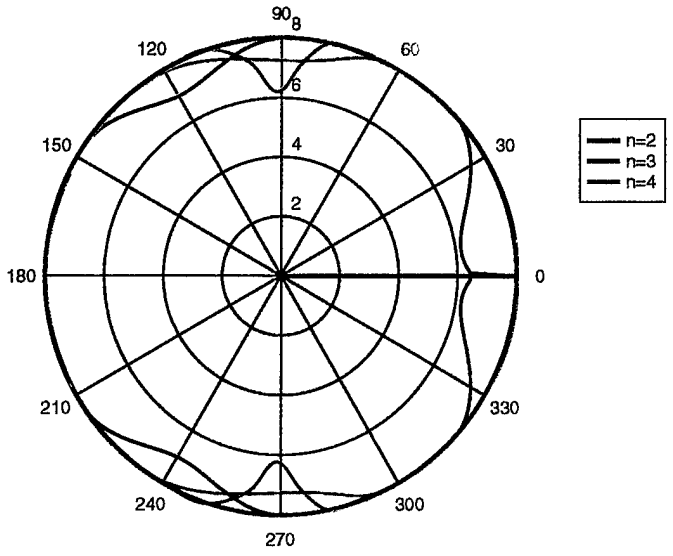

Figure 46. Sea state-polar plot, showing the effect of shape factors in limited length case, for U=8 Knots, h=2*D*.

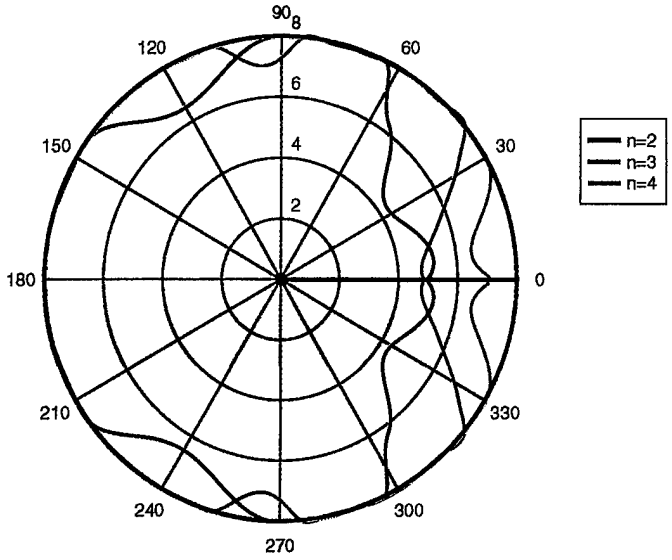

Figure 47. Sea state-polar plot, showing the effect of shape factors in limited diameter case, for U=11 Knots, h=2*D*.

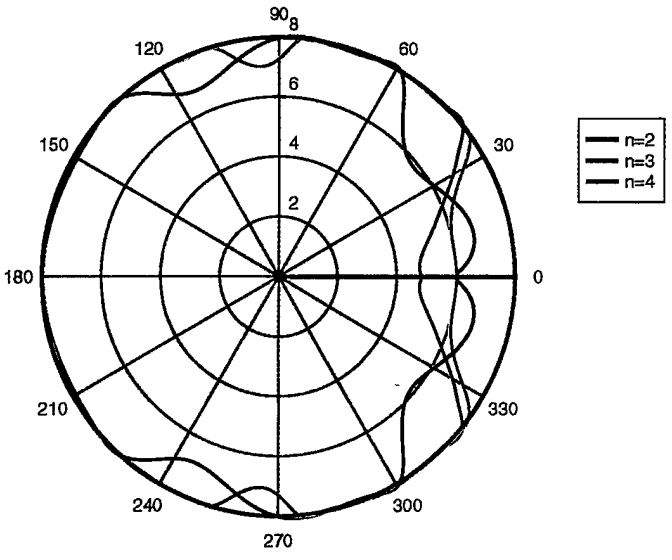

Figure 48. Sea state-polar plot, showing the effect of shape factors in limited length case, for U=11 Knots, h=2*D*.

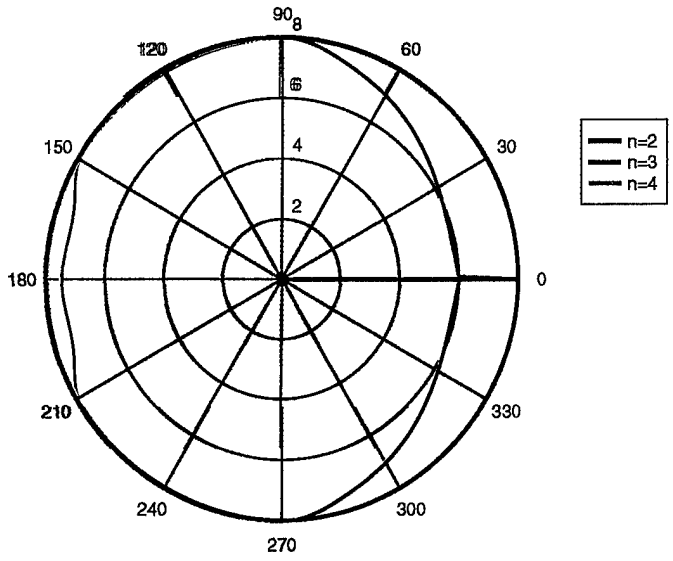

Figure 49. Sea state-polar plot, showing the effect of shape factors in limited diameter case, for U=3 Knots, h=2.5*D*.

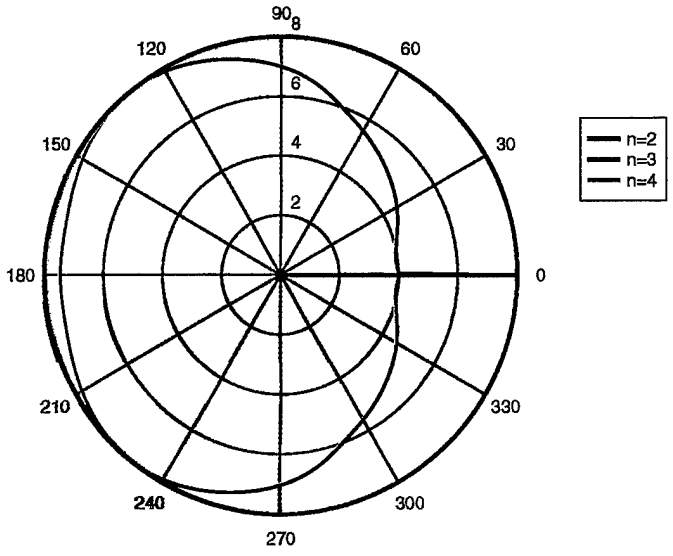

Figure 50. Sea state-polar plot, showing the effect of shape factors in limited length case, for U=3 Knots, h=2.5*D*.

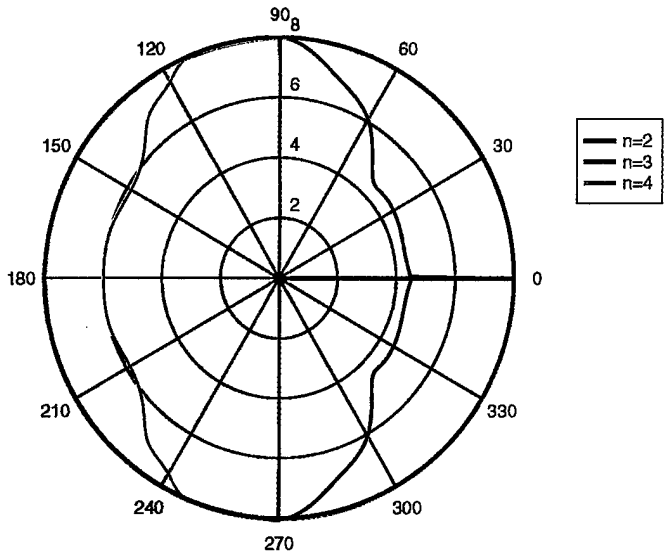

Figure 51. Sea state-polar plot, showing the effect of shape factors in limited diameter case, for U=5 Knots, h=2.5*D*.

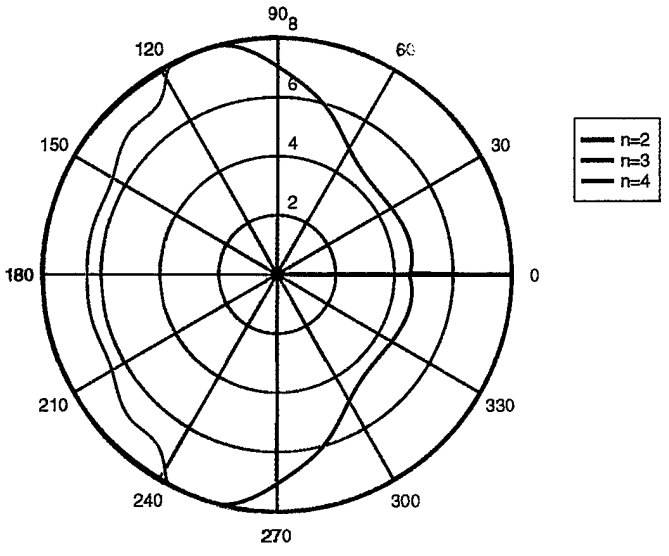

Figure 52. Sea state-polar plot, showing the effect of shape factors in limited length case, for U=5 Knots, h=2.5*D*.

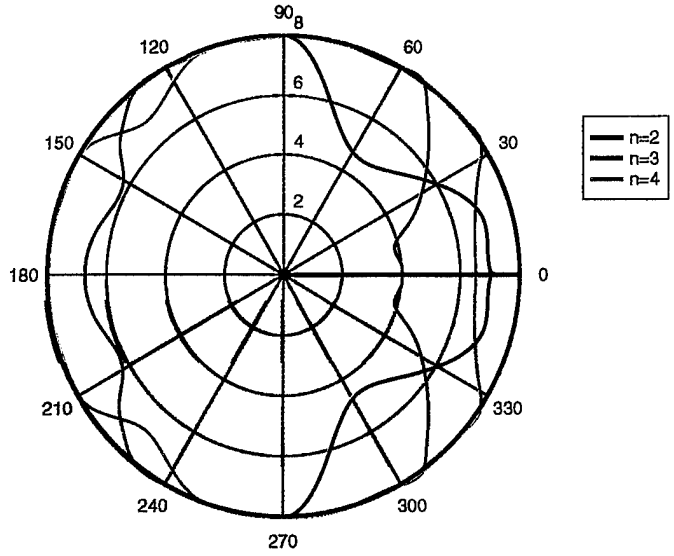

Figure 53. Sea state-polar plot, showing the effect of shape factors in limited diameter case, for U=8 Knots, h=2.5*D*.

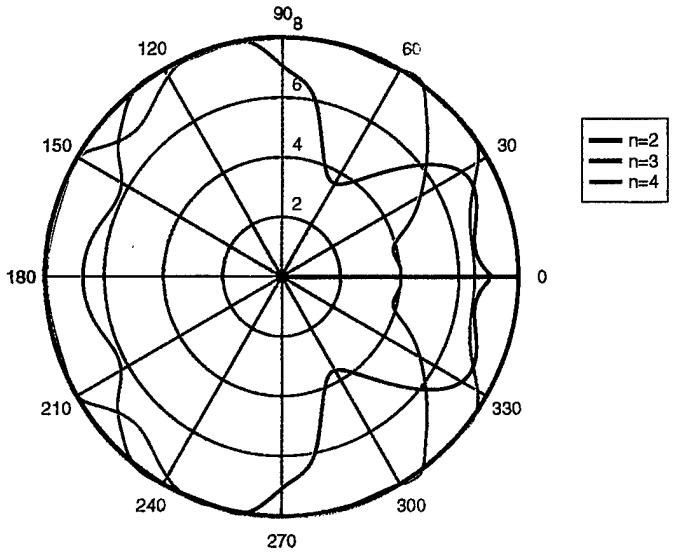

Figure 54. Sea state-polar plot, showing the effect of shape factors in limited length case, for U=8 Knots, h=2.5*D*.

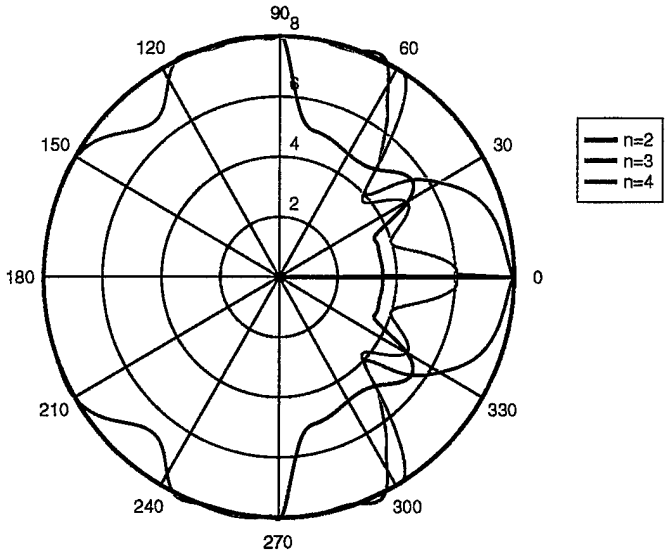

Figure 55. Sea state-polar plot, showing the effect of shape factors in limited diameter case, for U=11 Knots, h=2.5*D*.

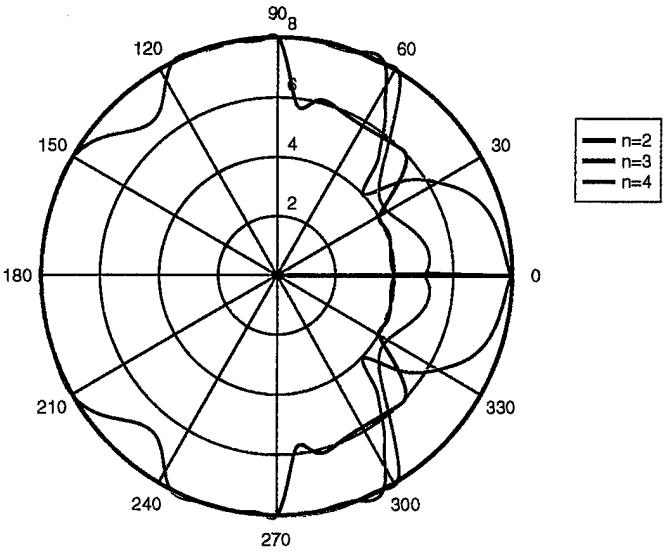

Figure 56. Sea state-polar plot, showing the effect of shape factors in limited length case, for U=11 Knots, h=2.5*D*.

D. COMBINED CRITERIA RESULTS

The operability indices for the combined criteria for the limited diameter and limited length cases in different speeds, operating depths and shape factors are shown in Tables V and VI, and in Figure 57. Typical polar plots are shown in Figures 58 through 81. Based on these results, the following conclusions can be drawn:

1.At smaller operating depths, varying the shape factors appear to yield a slight change in the number of expected criterion violations. At higher depths, smaller shape factors result in smaller operability indices.

2.Velocity has a little effect on the operability indices at smaller operating depths. As the depth increases, the indices appear to decrease with increasing speed.

		LIMITED DIAMETER			
		U=3	U=5	U=8	U=11
h=1.5D	n=2	0.4259	0.4259	0.4297	0.3085
	n=3	0.4694	0.4689	0.5067	0.4492
	n=4	0.5474	0.5107	0.4875	0.4976
h=2D	n=2	0.6236	0.6423	0.5307	0.3861
	n=3	0.5907	0.6030	0.5798	0.4959
	n=4	0.5238	0.5270	0.5179	0.5622
h=2.5D	n=2	0.5516	0.3744	0.4024	0.3116
	n=3	0.6382	0.6040	0.4760	0.4911
	n=4	0.6674	0.6342	0.5999	0.4293

Table V : Operability indices for combined criteria for the limited diameter case.

		LIMITED LENGTH			
		U=3	U=5	U=8	U=11
h=1.5D	n=2	0.4147	0.4295	0.4396	0.3974
	n=3	0.4694	0.4689	0.5067	0.4492
	n=4	0.4762	0.4772	0.4651	0.4638
h=2D	n=2	0.6461	0.6408	0.5286	0.4994
	n=3	0.5907	0.6030	0.5798	0.4959
	n=4	0.5334	0.5435	0.5676	0.5488
h=2.5D	n=2	0.4628	0.3560	0.3896	0.3247
	n=3	0.6382	0.6313	0.4760	0.4911
	n=4	0.6624	0.6312	0.5921	0.4347

Table VI : Operability indices for combined criteria for the limited length case.

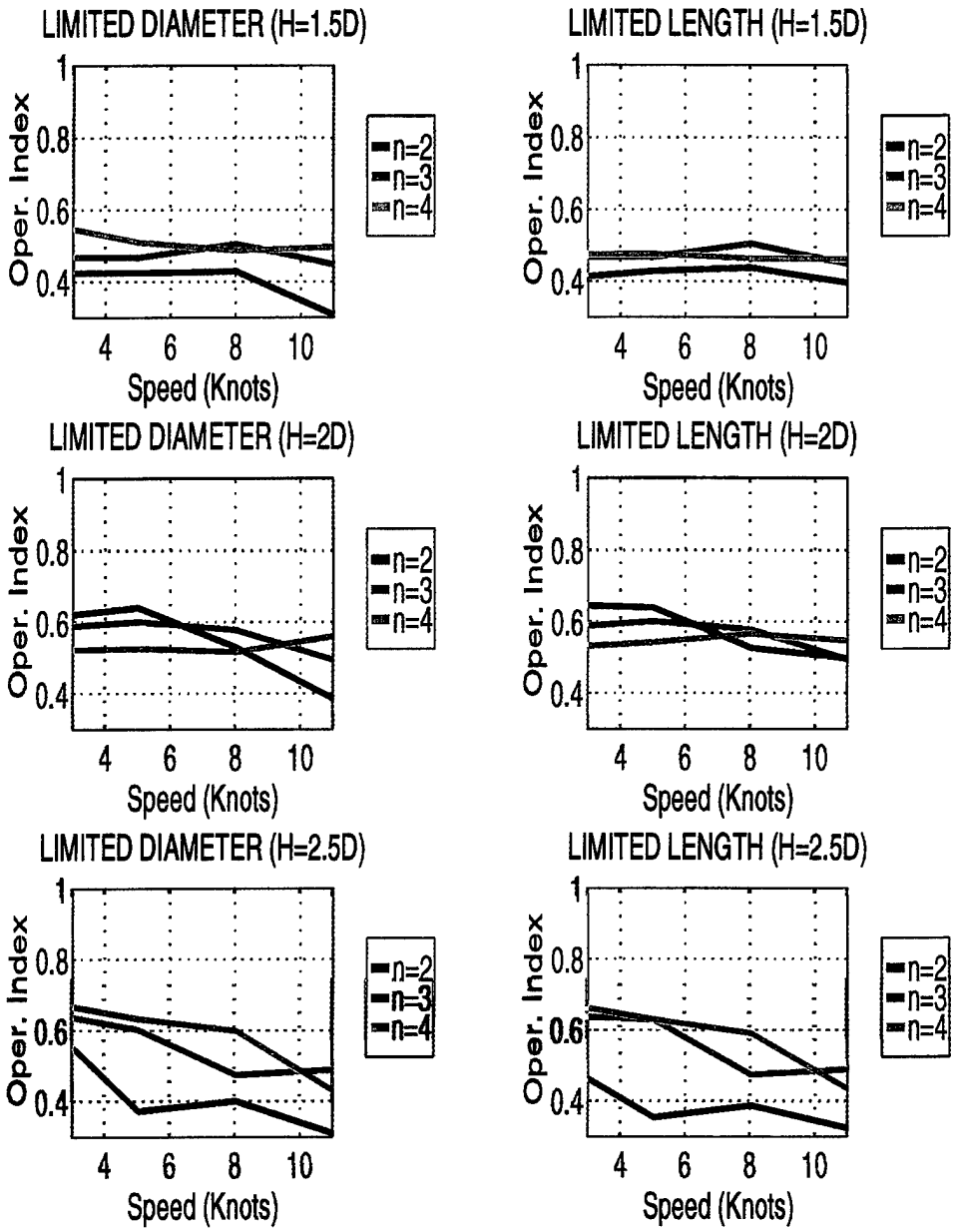

Figure 57. OI vs. submarine speed plots for combined criterion.

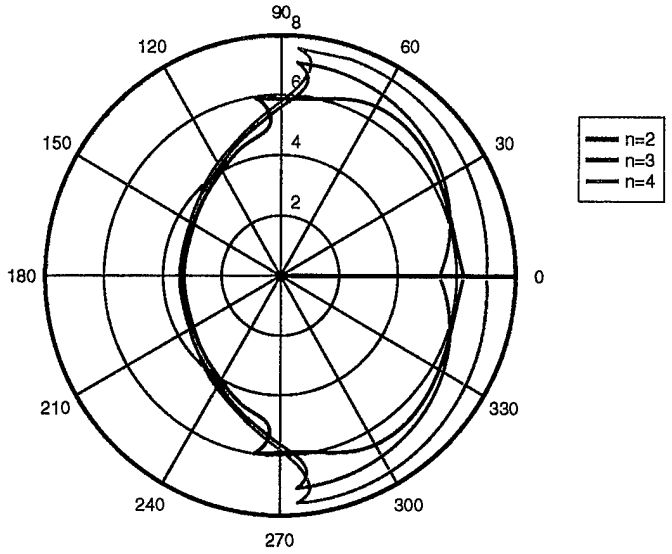

Figure 58. Sea state-polar plot, showing the effect of shape factors in limited diameter case, for U=3 Knots, h=1.5*D*.

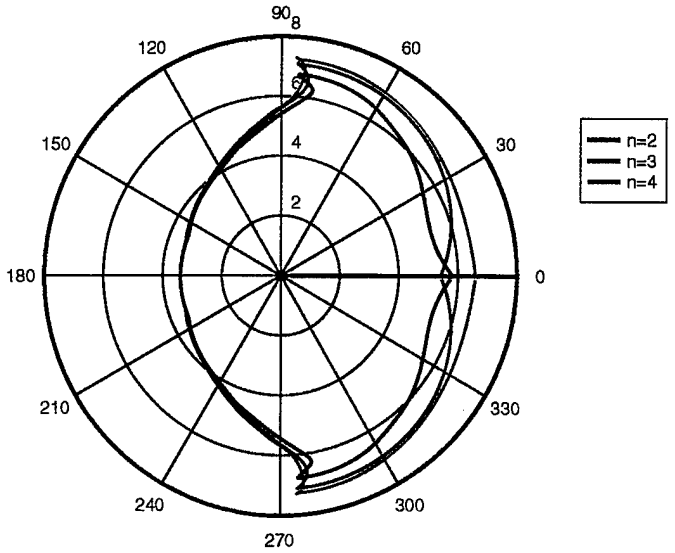

Figure 59. Sea state-polar plot, showing the effect of shape factors in limited length case, for U=3 Knots, h=1.5*D*.

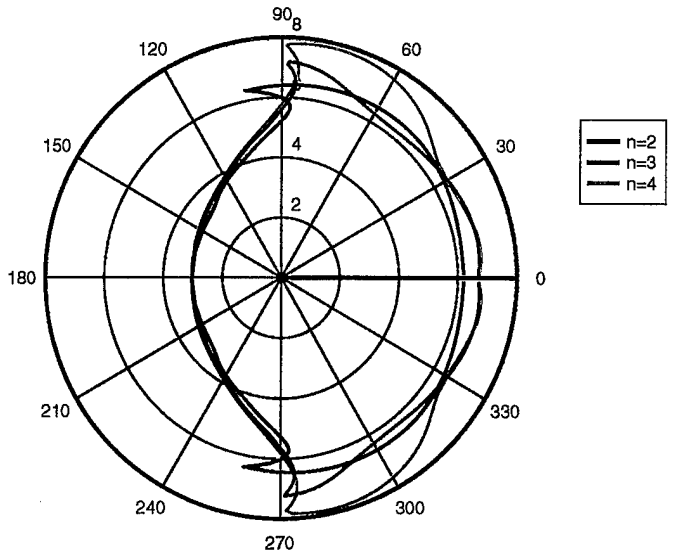

Figure 60. Sea state-polar plot, showing the effect of shape factors in limited diameter case, for U=5 Knots, h=1.5*D*.

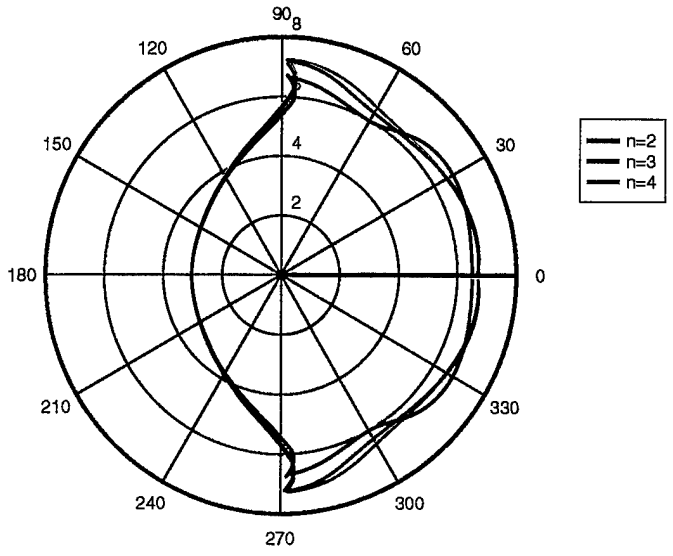

Figure 61. Sea state-polar plot, showing the effect of shape factors in limited length case, for U=5 Knots, h=1.5*D*.

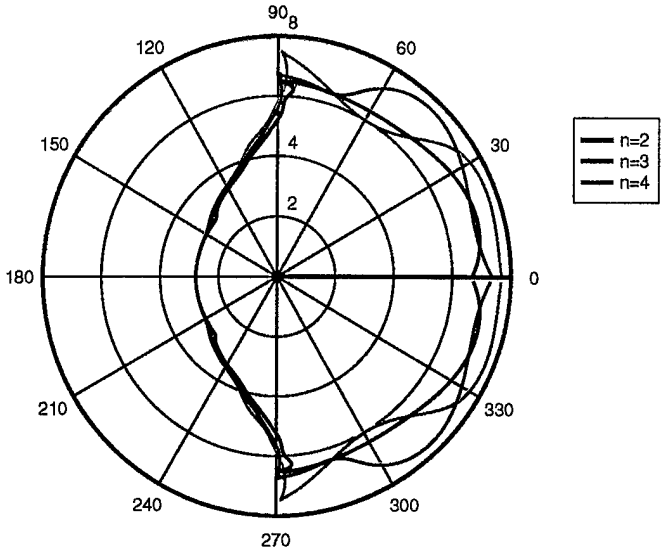

Figure 62. Sea state-polar plot, showing the effect of shape factors in limited diameter case, for U=8 Knots, h=1.5*D*.

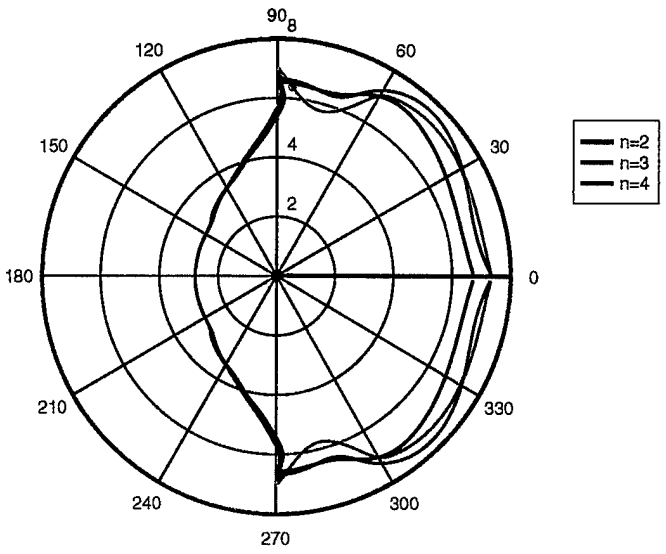

Figure 63. Sea state-polar plot, showing the effect of shape factors in limited length case, for U=8 Knots, h=1.5*D*.

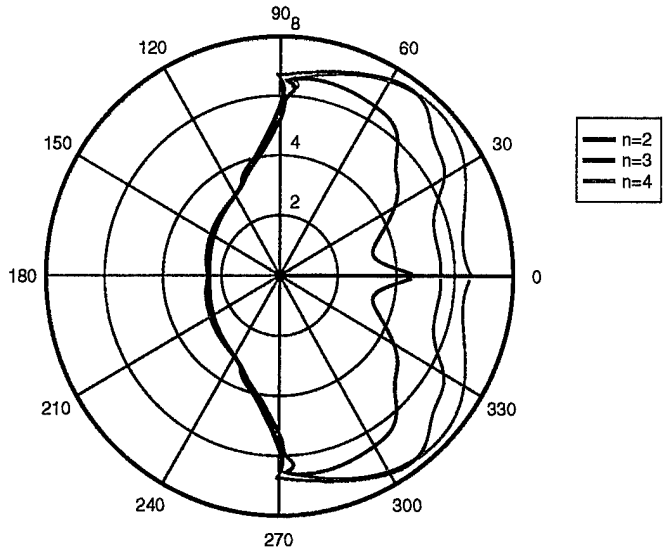

Figure 64. Sea state-polar plot, showing the effect of shape factors in limited diameter case, for U=11 Knots, h=1.5*D*.

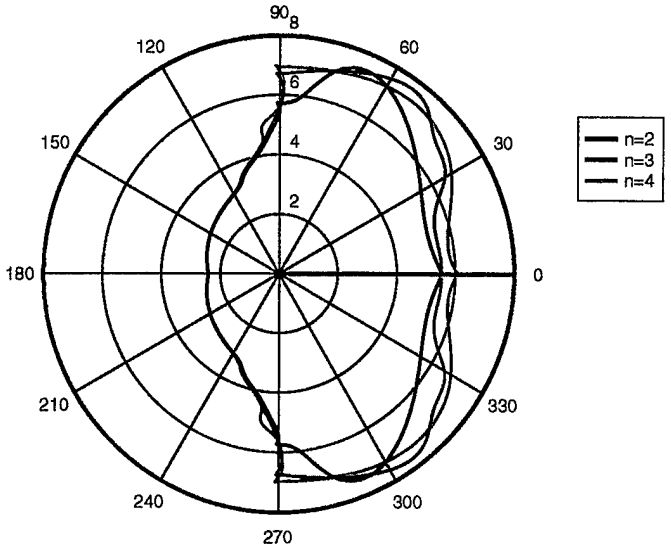

Figure 65. Sea state-polar plot, showing the effect of shape factors in limited length case, for U=11 Knots, h=1.5*D*.

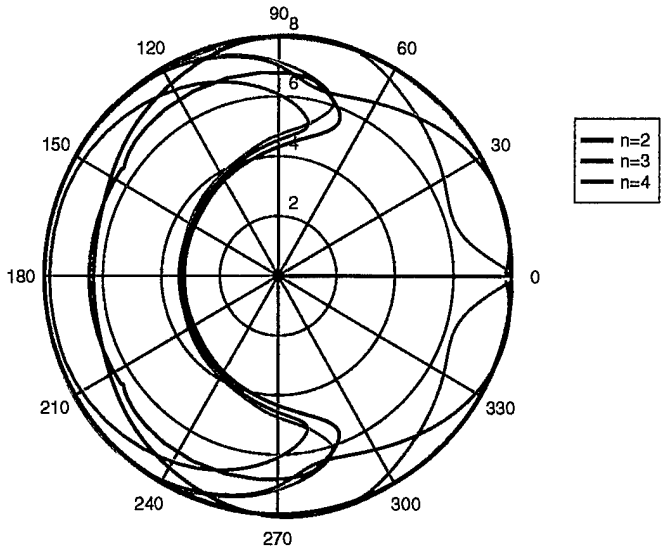

Figure 66. Sea state-polar plot, showing the effect of shape factors in limited diameter case, for U=3 Knots, h=2*D*.

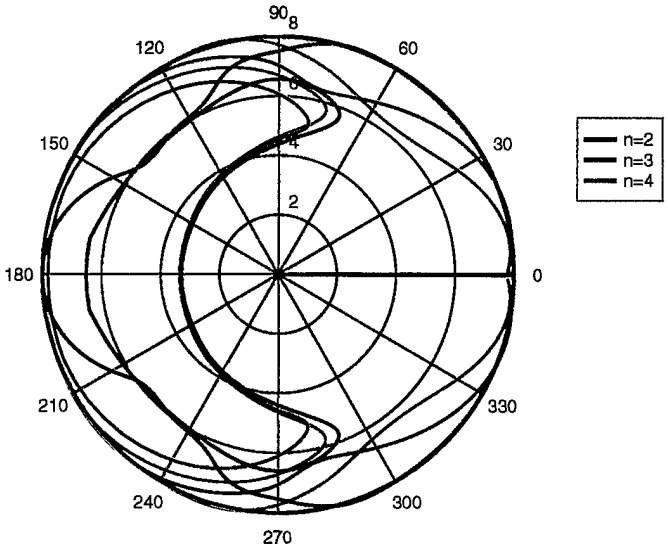

Figure 67. Sea state-polar plot, showing the effect of shape factors in limited length case, for U=3 Knots, h=2*D*.

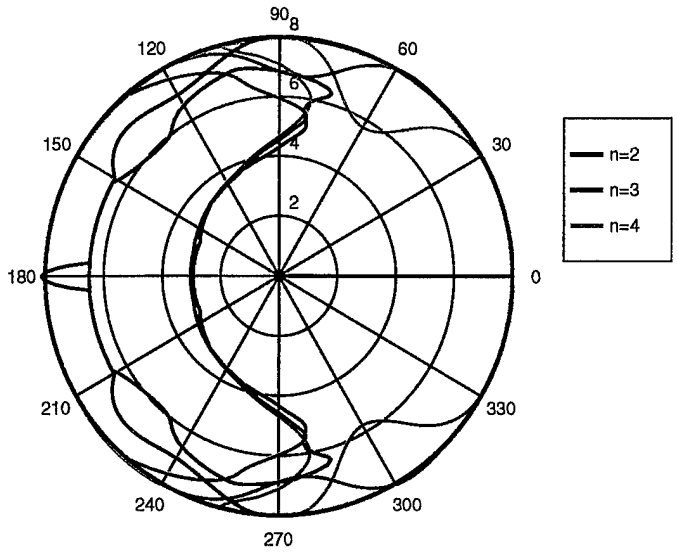

Figure 68. Sea state-polar plot, showing the effect of shape factors in limited diameter case, for U=5 Knots, h=2*D*.

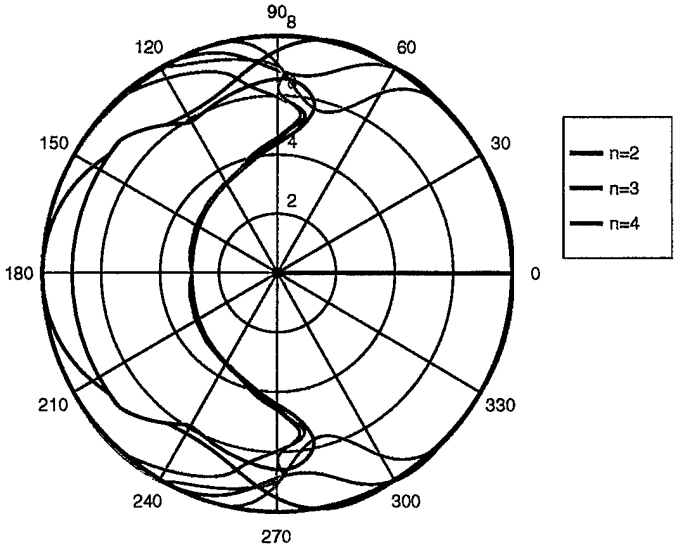

Figure 69. Sea state-polar plot, showing the effect of shape factors in limited length case, for U=5 Knots, h=2*D*.

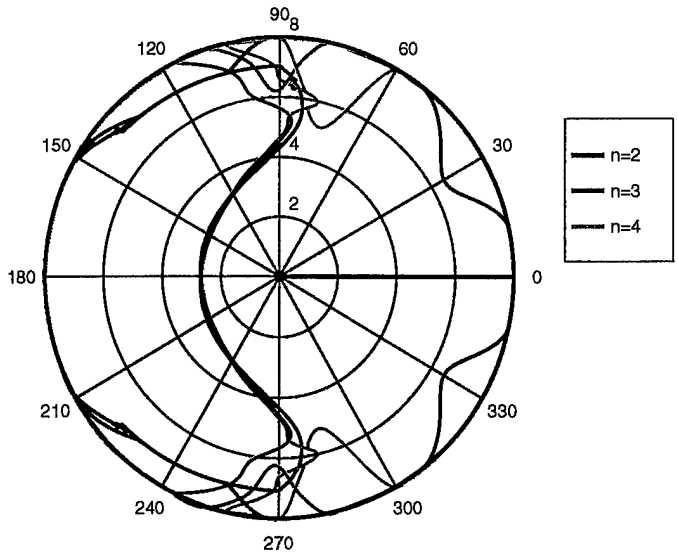

Figure 70. Sea state-polar plot, showing the effect of shape factors in limited diameter case, for U=8 Knots, h=2*D*.

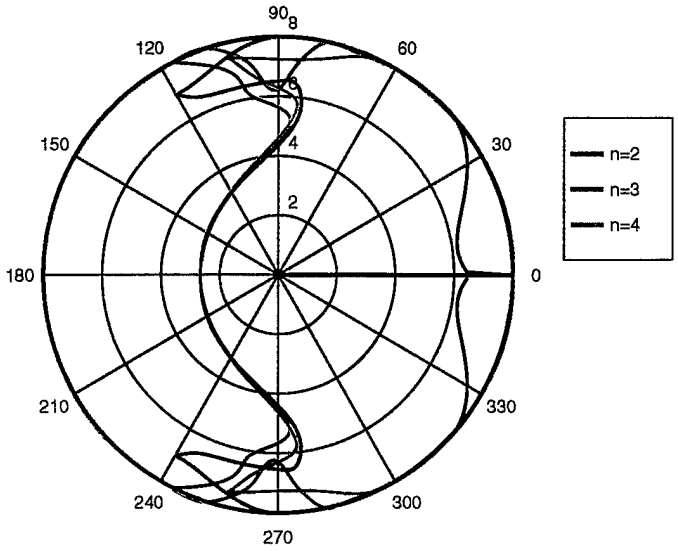

Figure 71. Sea state-polar plot, showing the effect of shape factors in limited length case, for U=8 Knots, h=2*D*.

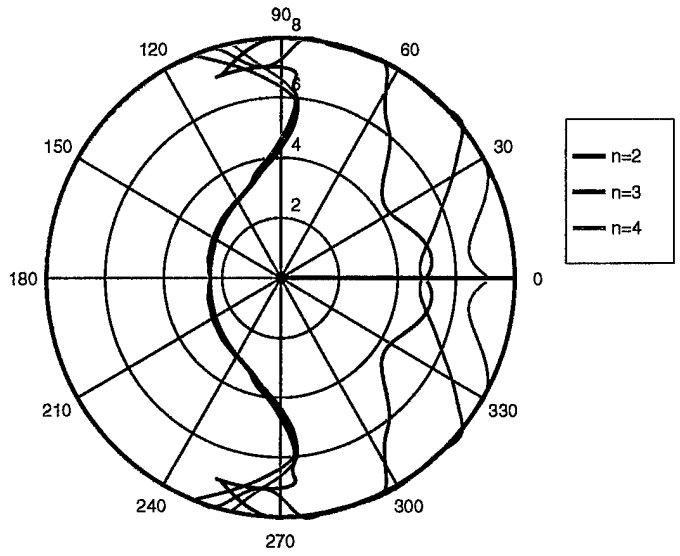

Figure 72. Sea state-polar plot, showing the effect of shape factors in limited diameter case, for U=11 Knots, h=2*D*.

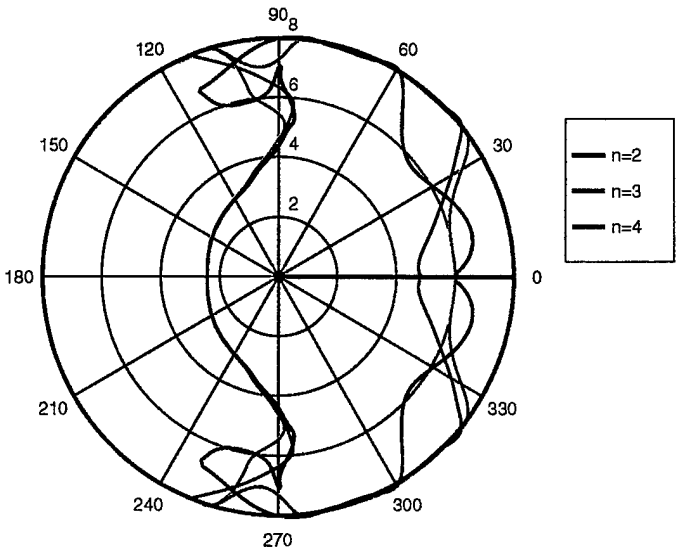

Figure 73. Sea state-polar plot, showing the effect of shape factors in limited length case, for U=11 Knots, h=2*D*.

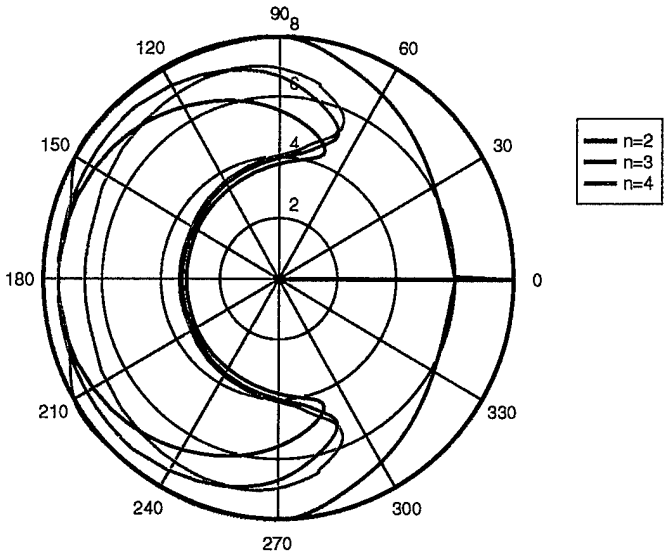

Figure 74. Sea state-polar plot, showing the effect of shape factors in limited diameter case, for U=3 Knots, h=2.5*D*.

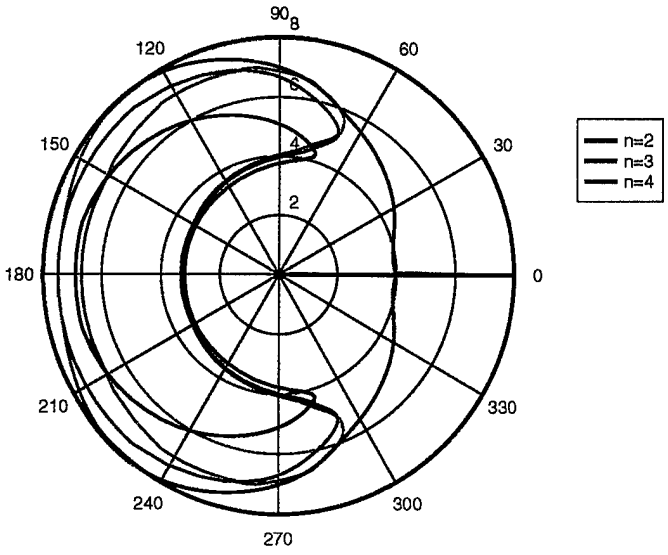

Figure 75. Sea state-polar plot, showing the effect of shape factors in limited length case, for U=3 Knots, h=2.5*D*.

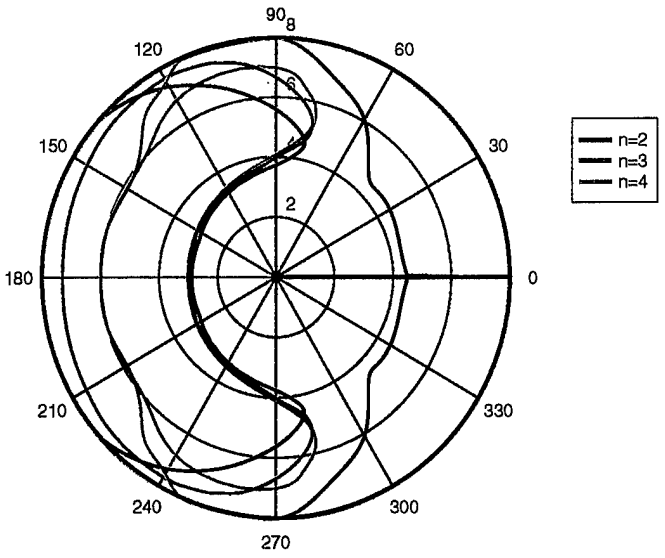

Figure 76. Sea state-polar plot, showing the effect of shape factors in limited diameter case, for U=5 Knots, h=2.5*D*.

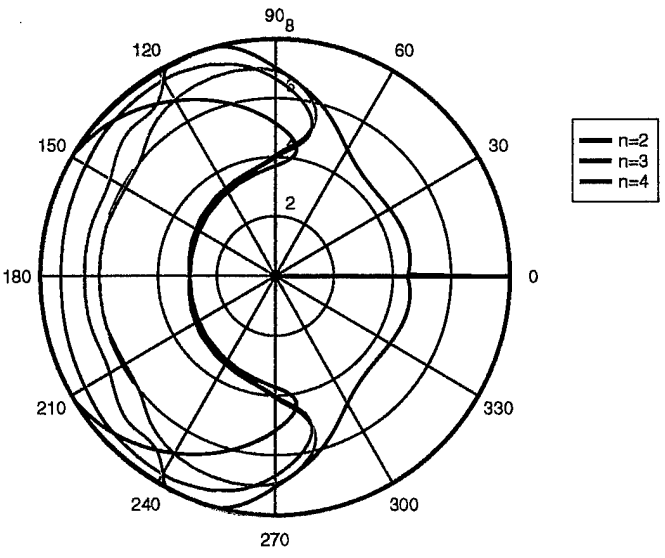

Figure 77. Sea state-polar plot, showing the effect of shape factors in limited length case, for U=5 Knots, h=2.5*D*.

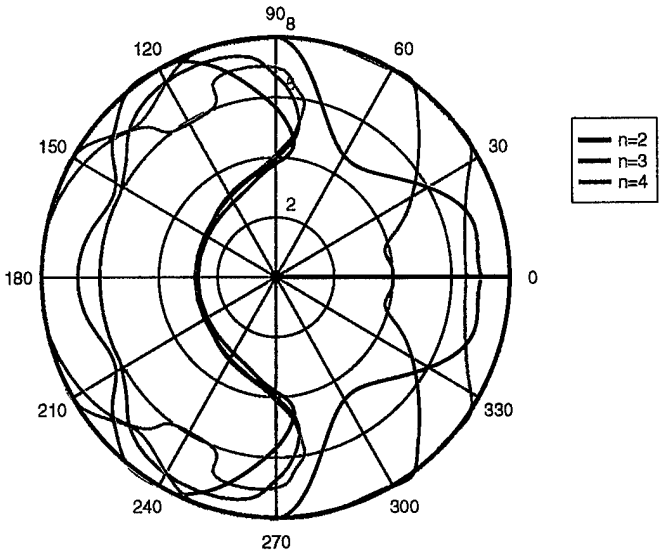

Figure 78. Sea state-polar plot, showing the effect of shape factors in limited diameter case, for U=8 Knots, h=2.5*D*.

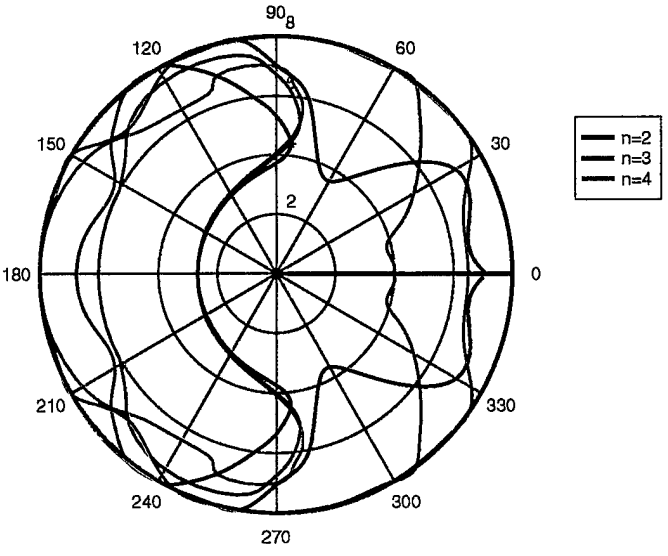

Figure 79. Sea state-polar plot, showing the effect of shape factors in limited length case, for U=8 Knots, h=2.5*D*.

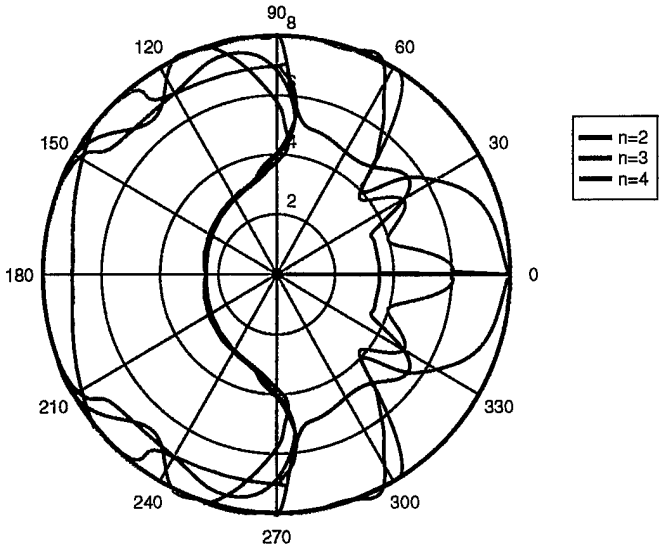

Figure 80. Sea state-polar plot, showing the effect of shape factors in limited diameter case, for U=11 Knots, h=2.5*D*.

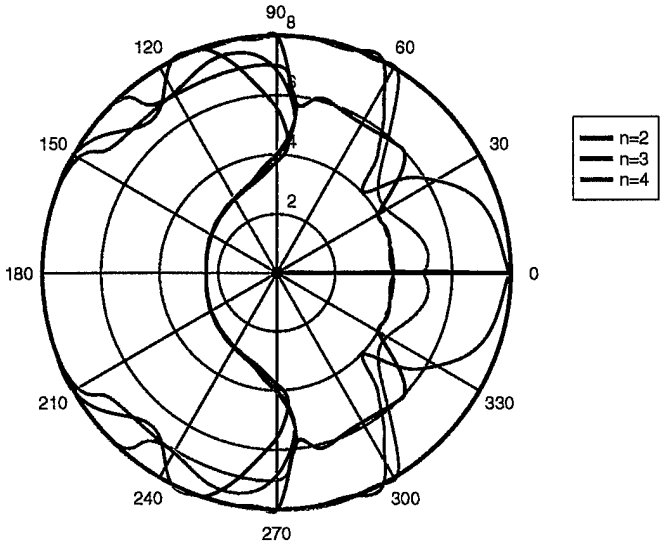

Figure 81. Sea state-polar plot, showing the effect of shape factors in limited length case, for U=11 Knots, h=2.5*D*.

IV. CONCLUSIONS AND RECOMMENDATIONS

A. CONCLUSIONS

In this research, the effect of geometric hull parameters, such as the length, the diameter and the shape factors of the hull, on the vertical plane response of submersible vehicles in the proximity of a free surface in deep water have been evaluated. Two cases, namely limited diameter and limited length, are considered, where in the first case overall length and in the second case the diameter is kept constant. The responses are evaluated by using a potential flow, strip theory solver for each case and for certain shape factors and different speed/operating depth combinations. Periscope submergence, sail broaching and the combination of both criteria are considered, in order to plot the operability envelope of the vehicle for different sea states and sea directions, using the above parameters. An operability index is calculated to quantify the operability of the vehicle. The main conclusions which are drawn from the study are shown below:

1. For the periscope submergence criterion, regardless of the variation of the parameters, head seas appear to result in a larger number of expected criterion violations than the following seas. Changes in the shape factors appear to have greater effects at smaller speeds and larger depths. An optimum shape factor for a certain operating depth, which minimizes the expected number of periscope submergence events can be found, and this appears to be a weak function of speed. Since the shapes of the operability envelopes can be quite different, similar values of the operability index may result in very different response characteristics.
2. For the sail broaching criterion, smaller shape factors generally yield smaller indexes. The operability index tends to increase as the depth increases, and in general, it is a

weak function of speed for all shape factors. The operability index does not appear to depend on sea direction consistently. At certain directions, the index decreases significantly for various shape factors and speed/depth combinations.

3. For the combined criterion, at smaller operating depths, changing the shape factors appears to yield a slight change in the number of expected criterion violations. At higher depths, smaller shape factors result in smaller operability indexes. Velocity has a little effect on the operability indexes at smaller operating depths. As the depth increases, the indexes appear to decrease with increasing speed.

B. RECOMENDATIONS

For further research on near surface response of submersible vehicles, the following studies are recommended:

1. In higher sea states for periscope submergence, even though the criterion is not violated, the average wave height may exceed the exposed periscope length, since the motion point appears to move more in phase with the incoming waves at higher sea states. This may cause difficulties in the operations, because the periscope moves in phase with the waves and the operator's visual horizon may be very small. Such situations should be analyzed with proper simulation studies.
2. Evaluating the effects of second order wave forces and motions on vehicle response. Even though these motions are slowly varying and can be controlled to a certain extent, they may alter both the values of the operability indices and the shape of the corresponding polar plots.

APPENDIX

PROGRAMS

In this Appendix, two Matlab programs for the limited diameter and the limited length cases and one Fortran program are presented. The purpose of the Matlab programs, as was mentioned in Chapter II, is to calculate the overall length for the limited diameter case, and the diameter for the limited length case. The programs take the shape factor values, n_a and n_f, as input and calculate the prismatic coefficients in both cases, the length in the limited diameter case, and the diameter in the limited length case. The Fortran program, DINIT.FOR, is used to create the necessary input file, SHIPMO.IN, for the strip theory seakeeping prediction program, SHIPMO.FOR [Ref. 2].The program reads the data written by the Matlab programs, and generates the input file, SHIPMO.IN.

```
% LIMDIA.M Limited diameter
%
% This program takes the shape factors, na and nf,
% as input, and calculates the corresponding
% length for the limited diameter case.

global na nf
d=30;
la=3.6*d;
lf=2.4*d;
v=217337.73;
na=input('Enter Na :');
nf=input('Enter Nf :');
xf=0:.3:lf;
xa=0:.3:la;
cpa=quad('funcpa',0,1,.001);
cpf=quad('funcpf',0,1,.001);
l=d*(4*v/pi/d^3-3.6*cpa-2.4*cpf+6);
bpl=l;
fid=fopen('LIM2DIN','w');
fprintf(fid,'%10.2f%10.2f%10.2f%10.2f\n',bpl,d,na,nf);
fclose(fid);
```

```
% LIMLEN.M Limited length
%
% This program takes the shape factors,na and nf,
% as input, and calculates the corresponding
% diameter for the limited length case.

global na nf
l=360;
la=108;
lf=72;
v=217337.73;
na=input('Enter Na :');
nf=input('Enter Nf :');

xf=0:.3:lf;
xa=0:.3:la;
cpa=quad('funcpa',0,1);
cpf=quad('funcpf',0,1);
c(1)=3.6*cpa+2.4*cpf-6;
c(2)=l;
c(3)=0;
c(4)=(-4*v/pi);
dr=roots(c);
d=dr(2);

la=3.6*d;
lf=2.4*d;

xf=0:.3:lf;
xa=0:.3:la;
cpa=quad('funcpa',0,1);
cpf=quad('funcpf',0,1);
c(1)=3.6*cpa+2.4*cpf-6;
c(2)=l;
c(3)=0;
c(4)=(-4*v/pi);
dr=roots(c);
d=dr(2);
bpl=l;

fid=fopen('LIM2DIN','w');
fprintf(fid,'%10.2f%10.2f%10.2f%10.2f\n',bpl,d,na,nf);
fclose(fid);
```

```
C-----------------------------------------------------------------------
C    DINIT.FOR
C
C     PROGRAM INITIALIZATION
C    This program generates the SHIPMO.INI file as an input file
C    for SHIPMO.FOR program.The variables are defined in the
C    program manual.
C -----------------------------------------------------------------------

      REAL BPL,LA,LF,PMB,D,NA,NF,XBKF,XBKA,BKWTH
      REAL RO,GRAV,GNU,CDISPL,DEPTH,XAXIS(21)
      REAL BILGRD,YAXIS(21,15),ZAXIS(21,15)
      REAL ZCG,RADGRO,CXCG,RADGYR,WANGI,WANGA,DWANG
      REAL XZNERT,XAC,YAC,ZAC,WA,SWL,BWL,DELWL
      REAL VMIN,VMAX,DELV,PARAM,FINISH,PI,NT,IS
      REAL XF(21),XA(21),YF(21),YA(21),CG
      INTEGER IA,IB,IC,ID,IE,IF,IG,IH,II,IJ,IK,IL,IN
      INTEGER NS,NPAC,I,ICALRD,ILID,NTO,NTI
      CHARACTER LABEL*80

      IA=0
      IB=0
      IC=1
      ID=2
      IE=0
      IF=0
      IG=0
      IH=1
      II=1
      IJ=0
      IK=0
      IL=0
      IN=0
      NS=21
      NPAC=1
      BKWTH=1.0
      XBKA=-10.0
      XBKF=10.0
      RO=1.9905
      GRAV=32.1740
      GNU=1.26E-05
      CDISPL=0.0
      DEPTH=0.0
      BILGRD=0.0
      ILID=0
      RADGRO=0.0
      CXCG=9999.0
      RADGYR=0.0
      XZNERT=0.0
      ICALRD=5
      FINISH=0.0
      PI=3.1415927
      NTO=15
      NTI=1
      WA=1.0
      SWL=0.2
      BWL=2.0
      DELWL=0.1
      WANGI=0.0
      WANGA=345.0
```

```
      DWANG=15.0

      BPL=360.0
      D=30.0
      NA=3.0
      NF=3.0

      VMIN=5*1.689
      VMAX=5*1.689
      DELV=0.0

      Z=2.5*D

      OPEN(10,FILE='SHIPMO.IN')
      WRITE(*,*)'ENTER LABEL'
      READ (*,'(A)') LABEL

      OPEN(100,FILE='LIM2DIN')
      READ(100,200) BPL,D,NA,NF

      LA=3.6*D
      LF=2.4*D
      PMB=BPL-6*D

      ZCG=(-1)*Z-(D/2)-3.0
      CG=(D/2)-3.0
      YAC=0.0
      XAC=(BPL/2.)-(BPL/3.)
      ZAC=(-1)*Z+D

      WRITE(*,*)'ENTER PARAM'
      READ *, PARAM1

      PARAM=PARAM1*3.28
      WRITE(10,*) LABEL
      WRITE(10,101) IA,IB,IC,ID,IE,IF,IG,IH,II,IJ,IK,IL,IN,NS,NPAC
      WRITE(10,1000) BPL,D,NA,NF,PARAM,Z,CG
      WRITE(10,102) BPL,RO,GRAV,GNU,CDISPL,DEPTH
      WRITE(10,103) XBKF,XBKA,BKWTH

      DO 11 IS=1,10
           XF(IS)=LF*(10-IS)/9
           XAXIS(IS)=(PMB/2)+XF(IS)
           YF(IS)=(D/2)*(1-(XF(IS)/LF)**NF)**(1/NF)
           DO 12 NT=1,7
                ZAXIS(IS,NT)=(-1)*Z-(D/2)-YF(IS)*SIN((PI/2)*(8-NT)/7.)
                YAXIS(IS,NT)=YF(IS)*COS((PI/2)*(8-NT)/7.)
12         CONTINUE
           ZAXIS(IS,8)=(-1)*Z-(D/2)
           YAXIS(IS,8)=YF(IS)
           DO 13 NT=9,15
                ZAXIS(IS,NT)=(-1)*Z-(D/2)+YF(IS)*SIN((PI/2)*(NT-8)/7.)
                YAXIS(IS,NT)=YF(IS)*COS((PI/2)*(NT-8)/7.)
13         CONTINUE
11    CONTINUE
      ZAXIS(10,15)=0.0
      YAXIS(10,15)=YF(10)*COS((PI/2)*(6./7.))
      XAXIS(11)=0.0
      DO 21 NT=1,7
           ZAXIS(11,NT)=(-1)*Z-(D/2)-(D/2)*SIN((PI/2)*(8-NT)/7.)
```

```
        YAXIS(11,NT)=(D/2)*COS((PI/2)*(8-NT)/7.)
 21CONTINUE
   ZAXIS(11,8)=(-1)*Z-(D/2)
   YAXIS(11,8)=D/2
   DO 31 NT=9,14
        ZAXIS(11,NT)=(-1)*Z-(D/2)+(D/2)*SIN((PI/2)*(NT-8)/7.)
        YAXIS(11,NT)=(D/2)*COS((PI/2)*(NT-8)/7.)
 31CONTINUE
   ZAXIS(11,15)=0.0
   YAXIS(11,15)=(D/2)*COS((PI/2)*(6./7.))
   DO 41 IS=12,21
        XA(IS)=LA*(IS-12.)/9.
        XAXIS(IS)=(-1)*(PMB/2)-XA(IS)
        YA(IS)=(D/2)*(1-(XA(IS)/LA)**NA)
        DO 42 NT=1,7
             ZAXIS(IS,NT)=(-1)*Z-(D/2)-YA(IS)*SIN((PI/2)*(8-NT)/7.)
             YAXIS(IS,NT)=YA(IS)*COS((PI/2)*(8-NT)/7.)
 42     CONTINUE
        ZAXIS(IS,8)=(-1)*Z-(D/2)
        YAXIS(IS,8)=YA(IS)
        DO 43 NT=9,15
             ZAXIS(IS,NT)=(-1)*Z-(D/2)+YA(IS)*SIN((PI/2)*(NT-8)/7.)
             YAXIS(IS,NT)=YA(IS)*COS((PI/2)*(NT-8)/7.)
 43     CONTINUE
 41CONTINUE
   WRITE(10,104) NTI,XAXIS(1),BILGRD,ILID
   WRITE(10,105) YAXIS(1,1),ZAXIS(1,1)
   DO 51 IS=2,20
        WRITE(10,104) NTO,XAXIS(IS),BILGRD,ILID
        DO 52 NT=1,15
             WRITE(10,105) YAXIS(IS,NT),ZAXIS(IS,NT)
 52     CONTINUE
 51CONTINUE
   WRITE(10,104) NTI,XAXIS(21),BILGRD,ILID
   WRITE(10,105) YAXIS(21,1),ZAXIS(21,1)
   WRITE(10,106) ZCG,RADGRO
   WRITE(10,107) CXCG,RADGYR,XZNERT
   WRITE(10,108) ICALRD,XAC,YAC,ZAC
   WRITE(10,109) WA,SWL,BWL,DELWL,VMIN,VMAX,DELV
   WRITE(10,110) WANGI,WANGA,DWANG
   WRITE(10,111) PARAM
   WRITE(10,112) FINISH

101FORMAT(15I5)
102FORMAT(3F10.4,2E15.5,F10.4)
103FORMAT(3F10.4)
104FORMAT(I5,2F10.4,I5)
105FORMAT(2F10.4)
106FORMAT(2F10.4)
107FORMAT(2F10.4,F15.3)
108FORMAT(I2,F8.4,2F10.4)
109FORMAT(8F10.4)
110FORMAT(3F10.4)
111FORMAT(F10.4)
112FORMAT(F4.1)
200FORMAT(4F10.2)
1000FORMAT(7F10.2)
   END
```

LIST OF REFERENCES

1. Crook, T. P., (1994), *An Initial Assessment of Free Surface Effects on Submerged Bodies*, M. S. Thesis, Naval Postgraduate School, Monterey, California.

2. Beck, R. F., and Troesch, A. W., (1989), *Documentation and User's Manual for the Computer Program SHIPMO.BM*, Report No. 89-2.

3. Jackson, H. A., (1992), *Fundamentals of Submarine Concept Design*, Proceedings SNAME Annual Meeting 1992 Paper No. 15.

4. Abramovitz, M., and Stegun, I. A., *Handbook of Mathematical functions*, Dover Publications, New York, 1970.

5. Papoulias, F. A.,(1993), *Dynamics of Marine Vehicles*, Informal Lecture Notes for ME4823, Naval Postgraduate School, Monterey, California.

INITIAL DISTRIBUTION LIST

		No. Copies
1.	Defense Technical Information Center 8725 John J. Kingman Rd., STE 0944 Ft. Belvoir, VA 22060-6218	2
2.	Dudley Knox Library Naval Postgraduate School 411 Dyer Rd. Monterey, California 93943-5101	2
3.	Chairman, Code ME Department of Mechanical Engineering Naval Postgraduate School Monterey, CA 93943-5000	1
4.	Professor Fotis A. Papoulias, Code ME/PA Department of Mechanical Engineering Naval Postgraduate School Monterey, CA 93943-5000	6
5.	Naval Engineering Curricular Office, Code 34 Naval Postgraduate School Monterey, CA 93943-5000	1
6.	Deniz Kuvvetleri Komutanlığı Personel Daire Başkanlığı Bakanlıklar, Ankara, Turkey	2
7.	Gölcük Tersanesi Komutanlığı Gölcük, Kocaeli, Turkey	1
8.	Taşkızak Tersanesi Komutanlığı Kasımpaşa, İstanbul, Turkey	1
9.	Deniz Harp Okulu Komutanlığı Tuzla, İstanbul, Turkey 81704	1
10.	İ. T. Ü. Gemi İnşa ve Deniz Bilimleri Fakültesi Kütüphanesi Maslak, İstanbul, Turkey 80626	1

11. M. Sadullah Öztürk 1
Büyükdere Cad. 28/A
Mecidiyeköy, İstanbul, Turkey

12. A. Kaan Çelikel 2
Altıntepe Eminalipaşa Cad. Köknar Sok.
Velidede Ap. D.9 81570
Küçükyalı, İstanbul, Turkey